The Hong Kong Polytechnic University
Department of Electrical Engineering

"Multiwavelength Fiber Ring Lasers"

TONG Fu Wa

A thesis submitted in partial fulfillment of the requirements for the Degree of Master of Philosophy

October 2002

CERTIFICATE OF ORIGINALITY

I hereby declare that this thesis is my own work and that, to the best of my knowledge and belief, it reproduces no material previously published or written nor material which has been accepted for the award of any other degree or diploma, except where due acknowledgement has been made in the text.

Signature : _____

Name : TONG Fu Wa

Acknowledgements

This thesis is dedicated to my mother who devotes much time to my education, health, and so on. Although she does not know how to teach me English, Physics, Mathematics and so on, I think her contribution on my life is great. I am greatly indebted for her encouragement.

In addition, I am pleased to express my gratitude to all teachers, classmates and persons who involved in my study and research projects. Following paragraphs are their images in my mind.

Dr. D. N. Wang is a responsible supervisor for my MPhil degree. He is enthusiastic about researches on the fiber lasers. His work on multi-wavelength pulse laser is worthy of praising. He gives me the freedom of my research. Frankly, when I was hindered by academic problems, I hesitated and felt frustrated. He taught me how to turn the problems into opportunities. After getting his encouragement at difficult periods, I can remind myself trying my utmost to achieve the goals.

Dr. W. Jin is my co-supervisor of MPhil degree, but his great impacts on my academic career and personal attitude are always deep in my heart. I met him when I was an undergraduate. With his patience and helpful hands, I gradually realized how to learn effectively, write sensibly and solve problems critically. By receiving his valuable advice, I succeeded in completing my final year project for the Bachelor Degree. He helped me strengthen the foundation in Fiber Optics. This paved a smoother way for my further study.

Dr. K. S. Lau, whom I met when I was an undergraduate, is a nice Associate Professor of Applied Physics. In my mind, he is an excellent teacher in the Wave and Optics. No matter how busy he was, he was willing to listen to and to teach me with patience. He taught me fundamental wave theories that I had never learned. His remarkable advice given to me surely benefited to the completion of my undergraduate final year project. Even I cannot meet him frequently, his influences on my study are obvious.

Dr. P. K. A. Wai is a well-known network expert. In my opinion, he looks like a mathematician and a physicist. I learned lots of theories about mathematical modeling, Soliton theory and network theories from him. He is familiar with optics and always

encourages me to raise questions. No matter how stupid the questions were, he was willing to give me answers with generous illustration. Certainly, I was benefited from his individual teaching.

Dr. K. H. Wong is one of the brilliant teachers in the Department of Applied Physics. Although he is busy with conducting researches on materials now, he made great contribution on the laser research before. By telling me work about famous physicists, such as Richard Feynman, their skills deeply impressed me. His famous note called Lecture on Lasers and their Application clearly directs me to think some challenging problems concerning the laser physics and the Quantum Mechanics. His teaching always triggers me to investigate the truth behind the lasers.

All in all, I would like to express gratitude to research assistants and my classmates who contributed to my work and gave me support, such as Dr. J. M. Gong, Dr. H. Li, Dr. L. Y. Simon Chan, Dr. H. L. Ho, Dr. W. H. Chung, Mr. Y. L. Hoo etc. Owing to their valuable inputs and ideas, I can finish my work successfully.

Fu Wa TONG

September 2002

Abstract

The main objective of this project is to build a multi-wavelength ring laser operated at room temperature. Multi-wavelength fiber laser sources have potential applications in optical communication systems and optical fiber sensing networks. The literature related to the fiber lasers is generally reviewed in order to understand the principle and the current development of the fiber lasers.

Essential optical components used in the multi-wavelength ring laser are discussed. They play important roles in the laser cavity. A Mach-Zehnder interferometer is used as the comb filter and its theoretical model is presented. By the use of an optical switch, the operating wavelengths can be shifted between two wavelength bands, centered at 1555 nm and 1565 nm respectively. Simultaneous operation of 10 wavelengths with wavelength spacing of 0.5 nm and SNR of 25 dB is demonstrated in an Erbium doped fiber ring laser having such a comb filter at 77 K.

The theoretical analysis and experimental investigation for the hybrid gain medium, which combines a homogeneous gain medium and an inhomogeneous gain medium, are carried out. Linearization, Perturbation Analysis and Stability Analysis are employed to obtain a theoretical model of the ring laser with the hybrid gain medium. A stable 22 wavelengths output from a hybrid gain laser with wavelength spacing of 0.5 nm and SNR of 25 dB is observed experimentally at room temperature.

Contents

Chapter 1

Introduction

1.1 The Aim

The aim of this thesis is to study a multi-wavelength fiber ring laser source operated at room temperature, to analyze roles of the major components in the multi-wavelength ring laser and to exploit possible configurations of the laser structures in order to enhance the flexibility in their operation and to increase the number of wavelengths in the lasing action. The theoretical analysis for the proposed configurations has been carried out in order to further understand the laser physics relevant to the multi-wavelength fiber laser and the results obtained in the analysis are verified by the experiments.

1.2 The Thesis Organization

In chapter 1, the state of the art of the optical fiber technology is generally reviewed. Challenges in telecommunication systems are stated. In fact, the multi-wavelength light sources play an important role in the optical communication system and optical fiber sensing system. Both systems are briefly introduced in the latter part of this chapter.

In chapter 2, the concise illustration on common laser models such as two level system and three level system is presented. Recent progress of multi-wavelength fiber lasers is briefly reviewed in order to provide a general research background.

In Chapter 3, the essential components in the multi-wavelength ring laser are investigated. These components play different roles in the laser cavity. A theoretical model of the comb filter called Mach-Zehnder interferometer is presented. Its functions are fully investigated in an experiment. Moreover, optical amplifiers such as Erbium Doped Fiber Amplifier (EDFA) and Semi-conductor Optical Amplifier (SOA) are discussed. Their amplification mechanisms are explained by means of the Two Level System and Three Level System.

In Chapter 4, the theoretical analysis and experiments about the hybrid gain medium, comprising the homogeneous gain medium and the inhomogeneous gain medium, are carried out. The Linearization, Perturbation Analysis and Stability Analysis are presented. The theoretical model of the ring laser with the hybrid gain medium is deduced. Such a ring laser is experimentally demonstrated to verify theoretically obtained results.

In Chapter 5, the major conclusion is made. The works worthy of further investigation are suggested.

1.3 The Beauty of the Optical Fiber Technology

The light guided by the glass is well known, but its power loss is tremendously large (1000 dB/km) in the glass. The glass was not a good transmission medium before. The lightwave communication in the glass was solely a dream. Until 1966, K. C. Kao and G. A. Hockham firstly proposed the low loss glass fiber as a transmission medium in telecommunication systems [1]. They claimed that the intrinsic loss of silica based glass was low enough to be a waveguide. The major loss was stemmed from the impurities such as high concentration of transition metal ions and hydroxyl. In 1970, Corning Glass Work proposed a method called Outside Vapor Deposition (OVD) to produce glass fiber with loss 20 dB/km successfully. In addition, the long-term stability about the semiconductor laser can be enhanced. Today, the dream of the lightwave communication really comes true.

Now, the loss of single mode fiber reduced to 0.2 dB/km. Consequently, the wide bandwidth around Infra-Red regions can be supported by the optical fiber. The first fiber, whose core and cladding diameters were 62.5 μm and 125 μm, was the multimode fiber. They facilitated the fiber fusion. The single mode fiber was prominent in long haul applications as it can support the transmission with high data rates. Its core diameter (9 μm) was an unique difference between the single mode and multimode fiber. Its bandwidth was higher than the bandwidth supported by the

multimode fiber due to the fact that the intermodal dispersion was absent in the single mode fiber.

There were two magic numbers (1.3 μm and 1.55 μm) in the optical communication. Around wavelengths at 1.3 μm and 1.55 μm were second and third communication windows respectively. The zero dispersion point can be found in the fiber at wavelength 1.3 μm. The wavelength with the lowest power loss of the fiber was 1.55 μm. Researchers did not satisfy the fiber with the zero dispersion point at 1.3 μm. After the waveguide technology was improved, the zero dispersion point shifted to 1.55 μm. The dispersion-shifted fiber, which simultaneously offered both the lowest power loss and zero dispersion characteristics at 1.55 μm, was developed [2].

In addition to the development of the fiber, the invention of the optical amplifiers called erbium doped fiber amplifier (EDFA) brightened the industry of the optical communication again. Since they can directly amplify optical signals without the conversions between photonic regime and electronic regime, their amplification was independent on the bit rates and data formats. Now, the optical signals can propagate through several hundreds kilometers long fiber networks by means of periodic optical amplification [3]. The transmission of multiple wavelengths was feasible within the gain spectrum of EDFA.

1.4 The Impacts on Telecommunication Networks Today

The traffic burden in the past telecommunication network was mainly voice signals rather than data signals. The practical frequency limitation of this network was a few Megahertz because intolerable loss with frequency dependence was introduced. Although coaxial cables with bandwidth of 10 GHz were developed to cope with bandwidth demanding problems, they were finally not the best transmission medium for high capacity networks. Yet, people were long for the networks having large capacity. The discussion on increasing challenges faced by the telecommunication industry realized the importance of DWDM (Dense Wavelength Division Multiplexing) devices and optical networking [4].

As the Internet users grew exponentially, the tremendous demand for the bandwidth capacity from the customers was inevitable. A long-distance carrier made a great progress in 1997 when it extended its bandwidth capacity to 1.2 Gbps (billions of bits per second) over a pair of the optical fibers. The transmission speed of 1 Gbps permitted to transfer 1000 books per second. This improvement on the transmission speed can support various applications such as Internet Phone, radio broadcast and so on. The network transmission rates of terabits (trillions of bits per second [Tbps]) were urged, which allowed to transmit 20 million simultaneous 2-way phone calls or the text from 300 year-worth of daily newspaper per second. The telecommunication

networks with such a transmission rate can carry the signals from different applications related to multimedia and video.

Frankly, it was hard to foresee the network growth for the purpose of meeting the market demand. A study estimated the demand on the U.S. interexchange carrier's network would increase sevenfold from 1994 to 1998, meanwhile the demand for the U.S. local exchange carrier's network would increase fourfold. A company pointed out its network growth was 32 times that last year, whereas another company said that the size of its network was double every six months within 4-year period [5].

1.5 Introduction to DWDM

The Dense Wavelength Division Multiplexing (DWDM) is an optical multiplexing technology. The number of wavelengths with a dense channel spacing ($\Delta \lambda$ <100 GHz) are coupled in a single optical fiber. This can dramatically increase the total bandwidth of the fiber. To cite an example, there are 10 wavelengths in the fiber. Each wavelength carries traffic at 10 Gbps rate. Finally, the aggregate bandwidth of the fiber is 100 Gbps. On top of this, each wavelength may also have different data formats and bit rates. This can allow the optical fiber to carry the optical signals with different traffic such as SDH, SONET and so on simultaneously [4,6].

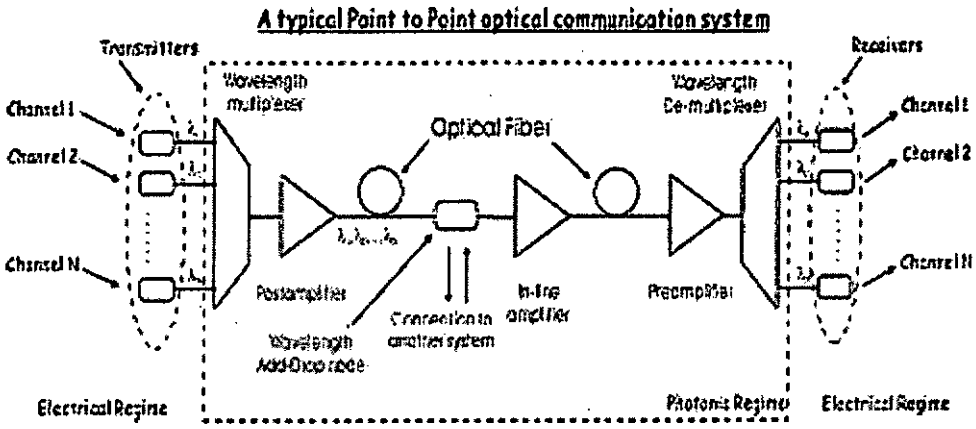

Fig. 1.1 The typical structure of optical communication system

Fig. (1.1) shows the typical "Point to Point" optical communication system in which there are different types of optical amplifiers, a wavelength multiplexer, a wavelength de-multiplexer, transmitters and receivers. In addition to those components, an add-drop node can be found to enable adding and dropping wavelength channels in an optical link.

In such optical communication systems, the electrical signals directly modulate to the optical wave in the transmitters by the use of Distributed Feedback (DFB) semi-conductor lasers. Different wavelength channels carrying optical signals are combined and sent to the optical fiber via the wavelength division multiplexer. Then, the optical amplifiers amplify the optical signals transmitted in different channels simultaneously in order to compensate the power loss stemmed from the transmission. The wavelength channels are de-multiplexed by using the wavelength de-multiplexer. Finally, the receivers convert the optical signals to the electrical signals.

In fact, the DWDM is able to cope with the shortage of the bandwidth of existing optical networks. The total bandwidth of the fiber is increased by two methods [4].

1. To increase the bit rate of each channel

   The bit rate of each channel increases from 2.5 Gbps to 10 Gbps. The channel capacity is 4 times larger than that before. On the one hand, this effectively increases the bandwidth of single channel. On the other hand, the cost effectiveness of the electronic circuits is quite low because their bit rate above 40 Gbps is a technical challenge.

2. To increase the number of wavelengths in the single fiber

   Several communication windows are defined for the transmission such as C-band (1530 nm-1560 nm), L-band (1570 nm-1620 nm) and so on. A number of wavelengths propagating through the fiber simultaneously are possible. If each channel carries the traffic with the same bit rate, the factor of increasing bandwidth will be only proportional to the number of wavelengths. Meanwhile, scientists were also concerned about the wavelength monitoring in the DWDM systems for the sake of system stability.

1.6 The FBG sensor systems based on multi-wavelength light sources

The invention of the Fiber Bragg Grating (FBG) is vital for the optical fiber sensing and the optical communication [7-8]. Since the FBG is compact and sensitive to the strain and temperature, the optical sensors based on the FBG were developed for many engineering applications such as structural monitoring and temperature sensing [3].

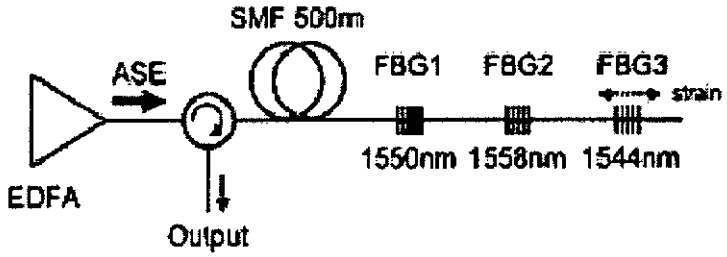

Fig. 1.2 A conventional passive FBG sensor head. SMF: Single Mode Fiber [9]

Fig. (1.2) shows a conventional passive FBG sensor system in which a broadband light source such as a Light Emitting Diode (LED) and the Amplified Spontaneous Emission (ASE) from the EDFA was utilized. The spectrum of the light source should cover the Bragg wavelength of the FBG [9]. Owing to weak optical power reflected by the FBG, the Signal to Noise Ratio (SNR) of such a system was limited [10-12].

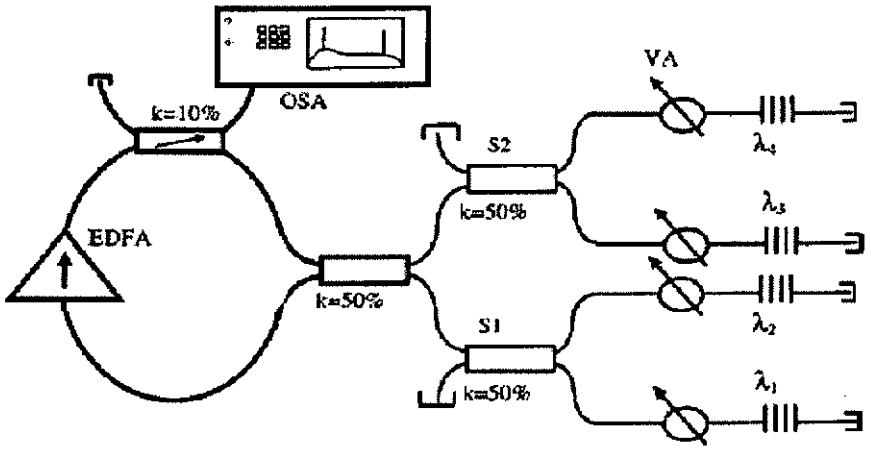

Fig. 1.3 An Erbium doped FBG fiber laser sensor. OSA: Optical Spectrum Analyzer, VA: Variable Attenuator [10]

Applying an Erbium doped fiber laser to the FBG sensor systems was intensively studied in Fig. (1.3) [10]. In fact, the FBGs act as sensor heads and reflectors of the laser cavity. This can successfully enhance the SNR of the sensor systems. Due to the homogeneous broadening of the Erbium doped fiber, there are only maximum 4 sensor heads in the fiber laser. Moreover, the output power of the fiber lasers fluctuates because of the serious mode competition between lasing modes.

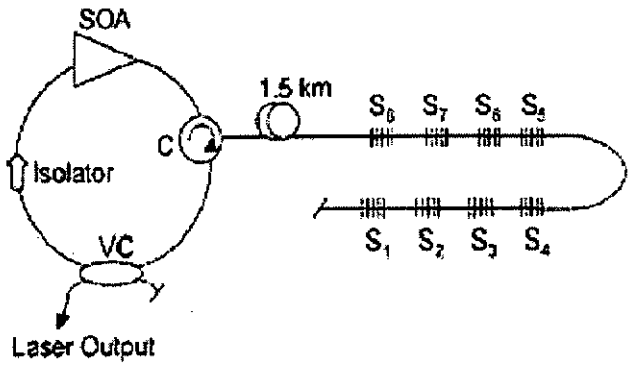

Fig. 1.4 A multi-wavelength FBG laser sensor system. SOA: Semiconductor Optical Amplifier, VC: Variable coupler [11]

Fig. (1.4) shows a multi-wavelength FBG laser sensor system. The number of sensing heads and SNR can be increased in such a system because the inhomogeneous property in the Semiconductor Optical Amplifier can support several lasing modes simultaneously [11]. The output power of the laser is stable.

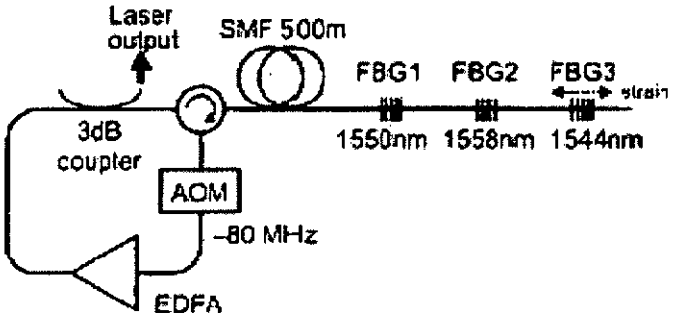

Fig. (1.5) A frequency-shifted multi-wavelength FBG laser sensor system. AOM: Acoustic optics modulator [12]

Fig. (1.5) shows frequency-shifted multi-wavelength FBG laser sensor system.

Owing to the breakthrough about the operation of multi-wavelength Erbium doped fiber laser at room temperature, the output power and SNR of the FBG sensor system are further enhanced [12].

1.7 The multi-wavelength light sources

The multi-wavelength light sources play an important role in the DWDM communication system and the optical fiber sensing system. The straightforward approach for building-up the multi-wavelength light source was to couple the wavelengths from an array of Distributed Feedback (DFB) lasers with individual wavelength directly modulated, which was called Array Lasers. Direct modulation of DFB lasers with modulation frequency of 2.5 GHz was performed.

The Multi-wavelength Fiber Ring Laser (MFRL) was also investigated. The main components of a fiber laser include gain media and comb filters. Multiple wavelengths were generated from the single light source. Each wavelength was de-multiplexed first by the demultiplexers. Then, the wavelengths were multiplexed after the modulation.

Although the individual DFB lasers can be modulated at very high speed, the array lasers have a coupler factor (1 / number of laser sources) coming from the coupler. For each of the DFB lasers used, an electronic driving circuit is needed. This is not cost effective. On top of this, the spacing between wavelengths is difficult to

maintain because the wavelength of the DFB laser may be changed by the age of the laser and mutual heating. There is also interchannel interference. Actually, MFRL also face the wavelength drifted caused by the comb filter, but the wavelength spacing is consistent. This can be settled down easily by the feedback control or good packaging [13].

1.8 References

1. K. C. Kao and G. A. Hockham, "Dielectric-Fiber surface waveguides for optical frequencies", *Proc. IEEE*, Vol. 133, No. 3, July 1966
2. G. Keiser, "Optical Fiber Communications", McGraw-Hill, Boston, 2000
3. A. M. Glass et al, "Advances in Fiber Optics", *Bell Labs Technical Journal*, pp. 168-184, Jan.-Mar. 2000
4. S. V. Kartalopoulos, "Introduction to DWDM technology: data in a rainbow", IEEE Press, New York, 2000
5. R. Ramaswami and K. Sivarajan, "Optical Networks: A practical perspective", Morgan Kaufmann Publishers, San Francisco, 1998
6. C. A. Brackett, "Dense wavelength division multiplexing networks: principles and applications", *IEEE J. Sel. Areas Commun.*, vol. 8, pp. 948-964, Aug. 1990
7. K. O. Hill and G. Meltz, "Fiber Bragg Grating Technology Fundamentals and Overview", *J. of Lightwave Technology*, vol. 15, no 8, Aug 1997, pp. 1263-1276
8. K. O. Hill, "Photosensitivity in Optical Fiber Waveguides: From Discovery to Commercialization", *J. on selected topics in Q. E.*, vol.6, no 6, Nov 2000, pp 1186-1189
9. A. D. Kersey, et al, "Fiber grating sensors", *J. Lightwave Technol.*, vol. 15, no. 8,

pp. 1442-1463, Aug. 1997

10. L. Talaverano, S. Abad, S. Jarabo and M. López-Amo, "Multiwavelength fiber laser sources with Bragg-grating sensors multiplexing capability", *J. Lightwav. Technol.* Vol. 19, No. 4, pp.553-558, April 2001

11. S. Kim, J. Kwon, S. Kim, B. Lee, "Multiplexed strain sensor using fiber grating-tuned fiber laser with a semiconductor optical amplifier", *IEEE Photon. Technol. Lett.*, vol. 13, No. 4, pp. 350-351, April 2001

12. S. Yamashita, T. Baba, K. Kashiwagi, "Frequency-shifted multiwavelength FBG laser sensor", *Optical Fiber Sensors Conference Technical Digest 2002*, pp. 285-288, 2002

13. M. Zirngibl, "Multifrequency lasers and applications in WDM networks", *IEEE Commun. Magazine*, Vol. 36, No. 12, pp.39-41, Dec. 1998

Chapter 2

Fiber Lasers and their lasing principles

2.1 Background

In this chapter, development of fiber lasers and their merits are presented first. Then, principles of lasers are described by the use of rate equations and the simple concepts of the fiber laser are also introduced. Finally, the recent progress of multi-wavelength fiber lasers is reviewed to provide a research background of the project.

Researches on the fiber lasers have been conducting for about four decades. Snitzer firstly reported experimental results about a Neodymium (Nd) doped glass fiber laser in 1961 [1]. Subsequently, researchers tried to find potential applications of fibers lasers. In 1966, Kao et al. proposed an attractive application of optical fiber related to telecommunication systems. This not only vitalized the communication systems but also revived the researches on the fiber lasers. Actually, optical fiber amplifiers are very important in the fiber lasers. In 1989, an Erbium Doped Fiber Amplifier (EDFA) was invented. It can be operated around 1550 nm corresponding to a spectral region with the lowest attenuation in an optical fiber. Then, different types of Erbium Doped Fiber (EDF) lasers were proposed, but they only operated at single

wavelength [2]. Because of bandwidth demanding in communication systems, Wavelength Division Multiplexing (WDM) can efficiently increase a transmission capacity of an existing optical communication system. A multi-wavelength light source can replace a lot of Distributed Feedback (DFB) lasers in WDM systems because it can simultaneously generate a number of wavelengths [3].

2.2 Benefits offered by fiber lasers

Fiber lasers are made by a rare earth doped optical fiber. The loss of optical fiber stemmed from scattering and absorption is very low. The optical components based on optical fibers facilitate alignment of fiber lasers. For example, we can utilize fiber couplers to perform a beamsplitting function in laser systems so that diffraction loss associated with bulk optic components can be avoided. In addition, all fiber reflectors, interferometers and resonators based on fiber coupler can be built easily. These not only decrease the power loss in laser cavities but also reduce the size of fiber lasers. Morcover, highly spatial overlap between pump power and lasing wavelength is expected in the single mode optical fiber to reduce the lasing threshold of the fiber lasers [4].

2.3 Recent progress of multi-wavelength fiber lasers

Multi-wavelength fiber lasers offer simultaneous operation of many wavelengths with fixed wavelength spacing. They have many applications ranging from dense wavelength division multiplexing (DWDM) optical fiber communication systems to optical fiber sensor networks. To satisfy wavelength spacing (0.8 nm) of the DWDM systems, an effect of cross saturation in a homogeneous broadening gain medium should be suppressed [5]. The wavelength range, over which cross saturation is effective, is determined by a homogeneous linewidth. At room temperature, the homogeneous linewidth of the EDF is at 10's of nm order. At 77 K, it is greatly reduced to 0.5-1.0 nm [5,6]. Then, the EDF becomes an inhomogeneous gain medium in which simultaneous operation of multiple wavelengths is allowed.

Park et al. made the first fiber laser generating 6 wavelengths [7]. The wavelength channels were separated by 4.8 nm. The linear cavity in the fiber laser was fabricated by splicing a WDM multiplexer to the EDF. Both fiber ends in the linear cavity were connected with two fiber loop mirrors. Although 6 different wavelengths were clearly found in an optical spectrum, a temporal modulation on a millisecond time scale was also observed. Actually, the modulation was come from a spatial hole burning, which can be avoided in an unidirectional ring laser. Six wavelength lasers with total output power of 1 mW were generated in such a ring laser. The average

power of each wavelength ranges from 50 to 150 μW.

Yamashita et al. first proposed to generate multi-wavelengths in the linear cavity EDF laser with a Fabry-Perot etalon at 77 K [8]. Only three lasing wavelengths with 0.8 nm wavelength spacing, which corresponded to the maximum transmission of the etalon, oscillated in the laser cavity at room temperature. Cooling EDF at 77 K can greatly increase the number of lasing wavelengths to 17 owing to strong suppression of the cross saturation at such a low temperature.

The laser cavity needs to include a WDM multiplexer or several filters to build a lot of possibly lasing modes in the multi-wavelength fiber laser. A filter with a comb like transmission spectrum can simplify the structure of the laser cavity. Ghera et al. took the advantage of a birefringence property of the optical fiber to form a comb filter [9]. A length of Polarization Maintaining (PM) fiber was introduced into a linear Nd-doped fiber laser in Fig. (2.1).

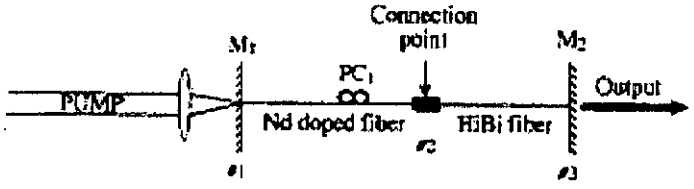

Fig. 2.1 Linear Nd-doped fiber laser had a length of PM fiber acting as a comb filter [9]

The PM fiber is actually a birefringent filter with the spacing between the

transmission peaks as illustrated in Eq. (2.1).

$$\Delta\lambda = \frac{\lambda^2}{2|n_s - n_f|L_{HiBi}} \tag{2.1}$$

Where

λ : An oscillating wavelength

$n_{s,f}$: Refractive indexes of the slow and fast birefringence axes of the PM fiber

L_{HiBi} : The length of PM fiber

At room temperature, four lasing wavelengths with a wavelength separation of 1 nm oscillated in the laser cavity with a PM fiber length of 1.2 m. Within same oscillation bandwidth, eight lasing wavelengths with wavelength spacing of 0.7 nm oscillated in laser cavity with a PM fiber length of 2 m.

In addition to the birefringence filter, an all fiber Fabry-Perot filter, whose Free Spectral Range (FSR) and fringe width were 0.09 and 0.03 nm respectively, was formed by two chirped Fiber Bragg Gratings (FBG) with a reflectivity of 50% which were separated by 8 mm. Chow et al. used this filter in the EDF ring laser at 77 K, which is shown in Fig. (2.2) [10]. Simultaneous operation of 11 wavelengths was achieved. Moreover, sampled FBG, which had a Fabry-Perot transmission spectrum with a FSR of 1.8 nm and a finesse of 15, was also introduced in the ring laser. It can facilitate the structure of the comb filter in the laser cavity. However, only five lasing wavelengths were generated in the EDF ring laser at 77 K because a number of

oscillating wavelengths was limited by a transmission bandwidth of the sampled FBG.

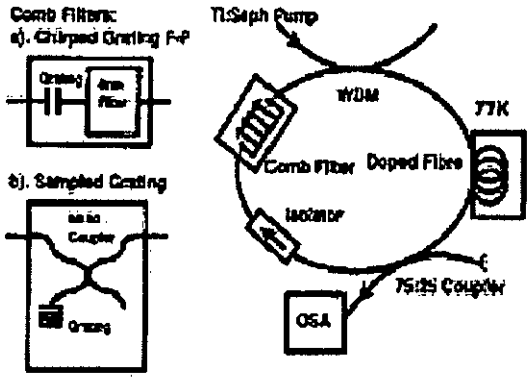

Fig. 2.2 An all fiber Fabry-Perot filter or sampled FBG were introduced in EDF ring laser [10]

The previous schemes on multi-wavelength generation is related to the EDF laser operation at 77 K. Cowle et al. proposed to use a hybrid gain medium in the fiber laser which can be operated at room temperature [11]. Fig. (2.3) shows a hybrid gain medium to include Brillouin gain and EDF gain. An optical pump source with a narrow linewidth excited the Brillouin gain in the optical fiber. It generated Brillouin signals in the optical spectrum by means of a Stimulated Brillouin Scattering effect. The frequency difference between the Brillouin signals was determined by an acoustic velocity in the optical fiber. In fiber laser with such a hybrid gain medium, simultaneous operation of multi-wavelength with wavelength spacing of 10.3 GHz was realized by continuously seeding the Brillouin signals to the Brillouin gain. The EDF gain only compensated the power loss in the laser cavity and increased output

power of the laser.

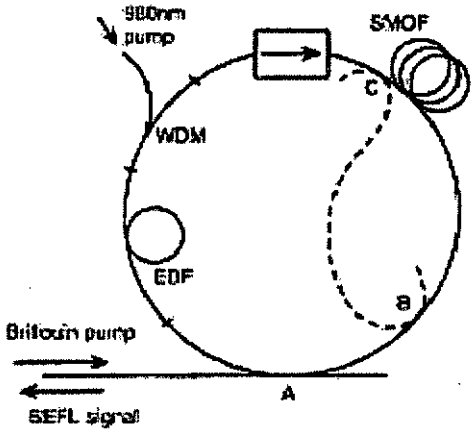

Fig. (2.3) The fiber laser had the hybrid Erbium/Brillouin gain medium [11]

Bellemare et al. suggested a frequency shifter working in the EDF ring laser cavity, which is shown in Fig. (2.4) [12]. The Amplified Spontaneous Emission (ASE) generated from the EDF circulated in the ring cavity. The period bandpass filter sliced ASE power on each circulation in order to ensure wavelength spacing of 0.8 nm. The ASE power on each circulation was frequency shifted by an acoustooptic frequency shifter in the laser cavity so that a steady state of a single mode oscillation was avoided. The EDF fiber lasers with frequency shifted feedback can allow 14 wavelengths to oscillate simultaneously. The Signal to Noise Ratio (SNR) and total power of the fiber laser were 20 dB and 7.8 dBm respectively.

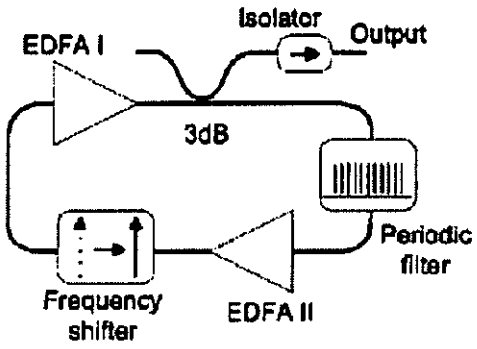

Fig. (2.4) The EDF fiber lasers with frequency shifted feedback [12]

2.4 Rate equations

Principles of lasing action are commonly explained by means of the rate equations. They seem to be a shortcut in analyzing the general performance of the lasers such as light intensity of each longitudinal mode. Actually, it is stemmed from the Semi-Classical Theory, but the descriptive explanation about the hole burning effect, mode competition and so on can be given [13]. The accurate characteristics of the quantum effects in the lasers cannot be found in such a theory. The simplification of the lasers can be achieved in the Two Level System and the Three Level System with descriptive presentation of energy levels and populations [14].

2.4.1 Two Level System

The Two level System was developed by Einstein in order to explain the concepts of spontaneous process and stimulated process. A hypothetical atom only having two

energy levels, E_1 and E_2, is considered. The energy level of E_1 is greater than that of E_2. N_1 and N_2 are the population density of the electrons in the lower and upper energy levels respectively in an unit volume. Then, the total population density is $N = N_1 + N_2$. Usually, the electrons always stay in the lower energy level of the atoms. Once a visible light source shines on the atoms, a lot of electrons in the lower energy level are excited to the upper energy level. This is called stimulated absorption which is proportional to N_1 and the photon flux density of the light source $\rho(\upsilon)$. Meanwhile, a few electrons in the upper level drop to the lower energy level. There are two types of radiative decay from the upper energy level to lower energy level; spontaneous emission and stimulated emission. The spontaneous emission always occur at an arbitrary rate A_{21} without stimulation. It is inversely proportional to the spontaneous life time. During the stimulated emission, incoming photons, whose energy value roughly equals $h\upsilon$, stimulate the electrons to fall on the lower energy level and to emit new photons with corresponding energy value. Fig. (2.5) shows the typical Two Level System.

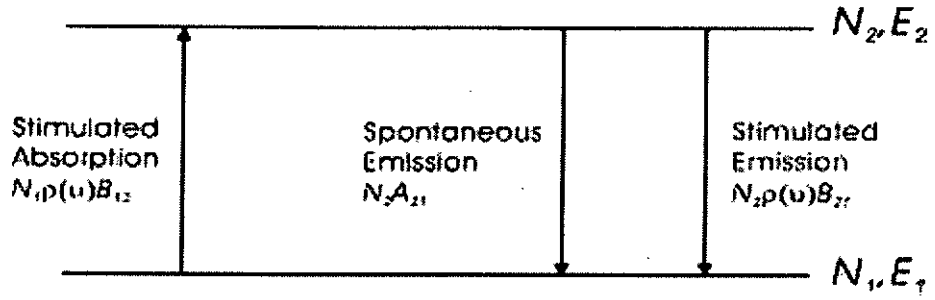

Fig. 2.5 The typical diagram of the Two Level System

The mathematical relationship in the lower energy level can be established. The rate equation of N_1 is given in Eq. (2.2)

$$\frac{dN_1}{dt} = -N_1\rho(\upsilon)B_{12} + N_2\rho(\upsilon)B_{21} + N_2A_{21} \qquad (2.2)$$

Where

N_1, N_2 : the population density of the electrons in the lower and upper energy levels

$\rho(\upsilon)$: the photon flux density

A_{21}: the spontaneous coefficient

B_{12},B_{21}: stimulated coefficients

At steady state, $\frac{dN_1}{dt} = 0$

$$N_1\rho(\upsilon)B_{12} = N_2\rho(\upsilon)B_{21} + N_2A_{21}$$

$$\rho(\upsilon) = \frac{A_{21}}{\frac{N_1}{N_2}B_{12} - B_{21}} \qquad (2.3)$$

Actually, the population density always obey Boltzman's distribution in Eq. (2.4) which is a typically classical statistics. h, υ, k *and* T are Planck's constant, frequency, Boltzman's constant and Temperature respectively.

$$\frac{N_1}{N_2} = e^{(E_2-E_1)/kT} = e^{h\upsilon/kT} \tag{2.4}$$

Then,

$$\rho(\upsilon) = \frac{A_{21}/B_{21}}{\frac{B_{12}}{B_{21}} e^{h\upsilon/kT} - 1} \tag{2.5}$$

B_{12} and B_{21} are assumed to approximately equal B in Eq (2.5). A_{21} is also replaced by A. The equation related to photon flux density is given in Eq. (2.6)

$$\rho(\upsilon) = \frac{A}{B(e^{h\upsilon/kT} - 1)} \tag{2.6}$$

$$\frac{N_2 A}{N_2 \rho(\upsilon) B} = (e^{h\upsilon/kT} - 1) \tag{2.7}$$

Eq. (2.7) shows that the possibility of the spontaneous emission is extremely higher than that of the stimulated emission because $h\upsilon/kT$ is about 80 at room temperature in visible region. In short, the population inversion impossibly occur in the Two Level System by means of optical pumping [13]. Then, the net gain of such a system is less than one. Nevertheless, the amplification supported by electrical pumping is still valid in the Two Level System because the excitation on electrons is based on the electrical pumping instead of the optical pumping.

2.4.2 Three Level System

Some lasers such as Ruby lasers and gas lasers were modeled by the Three Level System in which the stimulated emission can occur. Fig. (2.6) shows the schematic

diagram of such a system.

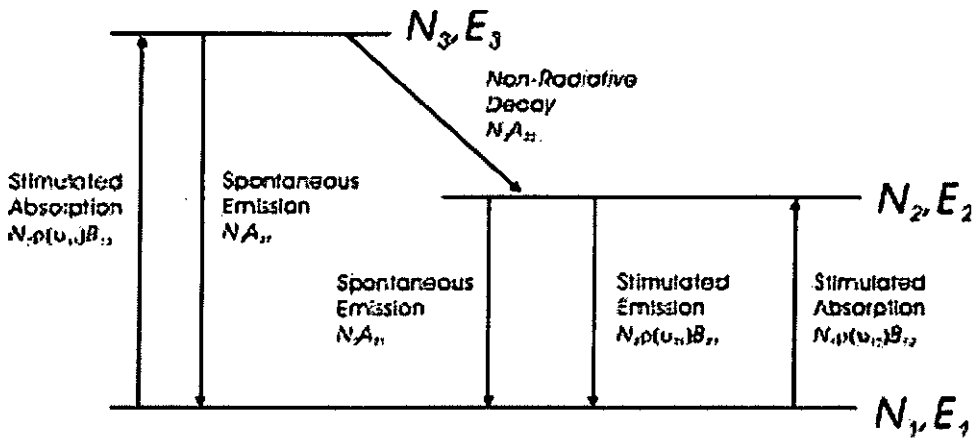

Fig. 2.6 The schematic diagram of the Three Level System

The rate equations in the three Level System are shown in Eq. (2.8-2.10). Eq. (2.11) shows the total population density.

$$\frac{dN_3}{dt} = N_1\rho(\upsilon_{13})B_{13} - N_3A_{32} - N_3A_{31} \tag{2.8}$$

$$\frac{dN_2}{dt} = N_3A_{32} + N_1\rho(\upsilon_{12})B_{12} - N_2\rho(\upsilon_{21})B_{21} - N_2A_{21} \tag{2.9}$$

$$\frac{dN_1}{dt} = N_3A_{31} + N_2A_{21} - N_1\rho(\upsilon_{13})B_{13} - N_1\rho(\upsilon_{12})B_{12} + N_2\rho(\upsilon_{21})B_{21} \tag{2.10}$$

$$N = N_1 + N_2 + N_3 \tag{2.11}$$

2.4.2.1 Before lasing action

If the equation related to the rate of change of photon flux density is considered, the analytical solution is not available. The solution of lasing action can only be obtained after numerically integrating the rate equations. However, the analytical

solution of the lasers before lasing action can be found. Before lasing action, the population density in the higher energy level approximately equals zero ($N_3 \approx 0$).

Within initial pumping, the stimulated process can be ignored except the stimulated absorption between the higher energy state and the ground state so that the spontaneous emission is mainly included in the rate equations. The simplified rate equations are shown in Eq. (2.12-2.14). The simplified total population density is given in Eq. (2.15). The factor of population inversion, *n(t)*, is defined in Eq. (2.16)

$$\frac{dN_3}{dt} \approx 0 \tag{2.12}$$

$$\frac{dN_2}{dt} = N_1 \rho(\upsilon_{13}) B_{13} - N_2 A_{21} \tag{2.13}$$

$$\frac{dN_1}{dt} = N_2 A_{21} - N_1 \rho(\upsilon_{13}) B_{13} \tag{2.14}$$

$$N = N_1 + N_2 \tag{2.15}$$

$$n(t) = \frac{N_2 - N_1}{N_2 + N_1} \tag{2.16}$$

Then, the *n(t)* can be determined after integrating Eq. (2.17). It is given in Eq. (2.18).

$$\frac{d(N_2 - N_1)}{dt} = 2 \times \left[N_1 \rho(\upsilon_{13}) B_{13} - N_2 A_{21} \right] \tag{2.17}$$

$$n(t) = m - (1+m) \exp\left\{ - \left[\rho(\upsilon_{13}) B_{13} + A_{21} \right] t \right\} \tag{2.18}$$

where

$$m = \frac{\rho(\upsilon_{13})B_{13} - A_{21}}{\rho(\upsilon_{13})B_{13} + A_{21}}$$

At t=0, $n(0)$=-1

At t=∞, $n(\infty)$=1

Now, $n(t)$ can be represented in Fig. (2.7). There is an absorption region which is below $n(t)$=0. The population inversion occur if $n(t)$ is greater than zero. Once the loss in the laser cavity equals the gain come from the population inversion, the lasing action occurs at the point called lasing threshold (γ_{th}). During the lasing action, the Eq. (2.18) is invalid.

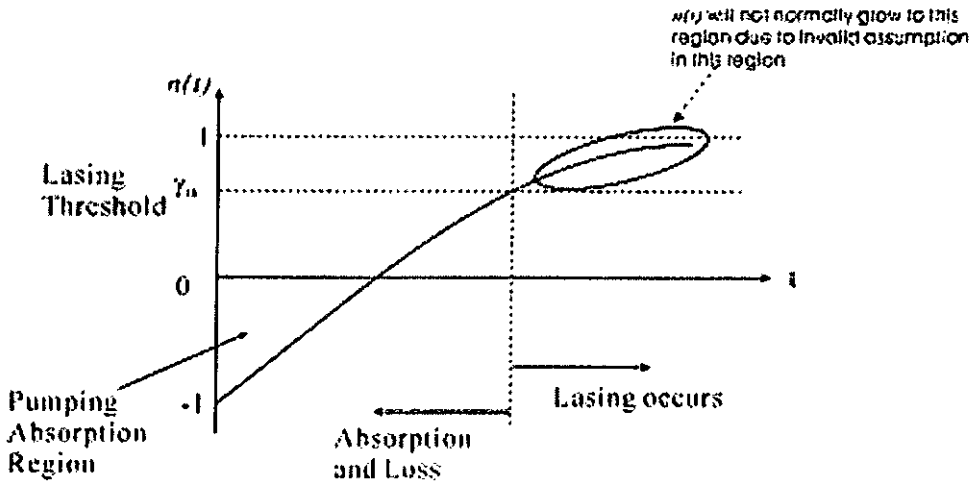

Fig 2.7 The population density before the lasing action

2.4.2.2 *After lasing action*

Once the lasers are operated above lasing threshold, there is a high photon flux density in the laser cavity. The interchange of energy between the photon flux and the

gain medium cause relaxation oscillation [15]. This phenomena is actually governed by a pair of coupled equations, which are given in Eq. (2.19) and (2.20).

$$\frac{d\Delta N}{dt} = S - \frac{\Delta N}{\tau} - \frac{\sigma}{h\upsilon}\Delta N I \tag{2.19}$$

$$\frac{dI}{dt} = \sigma \Delta N C I - \frac{I}{\tau_c} \tag{2.20}$$

where

ΔN : The population inversion, $N_2 - N_1$

S: The pumping rate

I: The light intensity of laser output

τ, τ_c : The time of spontaneous emission and photon life time in the laser cavity

σ : The effective cross section area of the laser

C: A constant

There is no analytical solution. A numerical solution of these equations can be found by a computational method. The relaxation oscillation is always a sinusoidally decaying laser output which is superimposed on a steady state intensity. Normally, the oscillation will be damped out after certain time which depend on the lifetime of the lasers. Finally, the lasers reach their steady state.

2.5 References

1. E. Snitzer, "Optical maser action of Nd^{3+} in a barium crown glass", *Phys. Rev. Lett.*, Vol. 7, pp.444-446, 1961
2. S. Yamashita, "Recent Advances and Applications of Fiber Lasers", *OECC 2002*, pp. 630-631, July 2002
3. M. Zirngibl, "Multifrequency lasers and applications in WDM networks", *IEEE Commun. Magazine*, Vol. 36, No. 12, pp.39-41, Dec. 1998
4. P. Urquhart, "Review of rare earth doped fibre lasers and amplifiers", *IEE Proceedings J.* , Vol. 135, pp. 385-407, Dec. 1988
5. M. J. F. Digonnet, "Rare-Earth-Doped Fiber Lasers and Amplifiers", Second Edition, Marcel Dekker Inc., New York, 2001
6. J. L. Zyskind et al., "Determination of homogeneous linewidth by spectral gain hole-burning in an Erbium-Doped Fiber Amplifier with GeO_2:SiO_2 core", *IEEE Photon. Technol. Lett.*, Vol. 2, No. 12, pp. 869-871, Dec. 1990
7. N. Park et al., "Multiple wavelength operation of an erbium-doped fiber laser", *IEEE Photon. Technol. Lett.*, Vol. 4, No. 6, pp. 540 -541, June 1992
8. S. Yamashita and K. Hotate, "Multiwavelength erbium-doped fibre lasr using intracavity etalon and cooled by liquid nitrogen", *Elect. Lett.*, vol. 32, No. 14, pp. 1298-1299, July 1996

9. U. Ghera et al., "A fiber laser with a comb-like spectrum", *IEEE Photon. Technol. Lett.*, Vol. 5, No. 10, pp. 1159-1161, Oct. 1993

10. J. Chow et al., "Multiwavelength generation in an erbium-doped fiber laser using in-fiber comb filters", *IEEE Photon. Technol. Lett.*, Vol. 8, No. 1, pp.60-62, Jan. 1996

11. G. J. Cowle and D. Yu. Stepanov, "Multiple wavelength generation with Brillouin/erbium fiber lasers", *IEEE Photon. Technol. Lett.*, Vol. 8, No. 11, pp. 1465-1467, Nov. 1996

12. A. Bellemare et al., "Room temperature multifrequency erbium-doped fiber lasers anchored on the ITU frequency grid", *J. Lightwav. Technol.*, Vol. 18, No. 6, pp. 825-831, June 2000

13. W. Silfvast, "Laser fundamentals", Cambridge University Press, Cambridge, 1996

14. A. E. Siegman, "Lasers", University Science Books, Mill Valley CA, 1986

15. K. Shimoda et al., "Introduction to laser physics", Springer-Verlag, Berlin, 1986

Chapter 3

Essential Elements of Multi-Wavelength Fiber Ring Laser

3.1 Background

Equipment in the Dense Wavelength Division Multiplexing (DWDM) transmission was widely deployed in the long haul communication systems last few years. Current communication systems utilize 8 or 16 wavelength channels [1-2]. They can carry signals with different bit rates. Each channel is generated by a semi-conductor diode such as a Distributed Feedback (DFB) laser. Owing to the bandwidth demand in telecommunication networks, the number of wavelengths launched to an optical fiber should be as many as possible in the future so as to increase the transmission capacity of the networks. There is no denying that manufacturing and maintaining the large number of laser diode is very costly and inefficiently. A device, which can generate multiple wavelengths simultaneously, is highly desirable in the telecommunication networks. This also triggers research interests related to the operation of the Multi-Wavelength Fiber Lasers.

In this chapter, the essential components in the Multi-Wavelength Fiber Ring Laser (MFRL) such as optical amplifiers and comb filters are briefly introduced. In

addition, the detailed functions of the comb filter in MFRL are studied both theoretically and experimentally in the latter part of this chapter.

3.2 Optical Amplifiers

When the optical signals propagate along the optical fiber, they suffer from the loss. In order to maintain the minimum Signal to Noise Ratio (SNR) required by communication systems, repeaters should be installed between signal sources and receivers. There are two kinds of the repeaters; Regenerators and Optical Amplifiers.

The regenerator includes an optical receiver, an electrical amplifier and an optical transmitter. It is responsible for lots of tasks such as retiming, error recovery, amplification, pulse reshaping and so on [2-3]. In spite of above attractive features, the regenerator cannot be widely used in the multi-wavelength optical communication systems because it only amplifies the optical signal with a single wavelength. Actually, a number of regenerators have to be applied to the multi-wavelength optical communication systems so that the amplification of multi-wavelength signals can be carried out simultaneously. This seems feasible in the systems with several wavelengths and moderate speed. Nevertheless, the maintenance cost is significantly high in high speed optical networks. In addition, the optical signals are converted to the electrical signals in the regenerators first. After signal processing in the electrical

domain, the regenerator transmits the optical signals to the optical fiber. Such processes are time consuming. The regenerators always cause "bottleneck" problems in the high speed optical networks.

Recently, Raman Optical Amplifier (ROA), Semi-conductor Optical Amplifier (SOA) and Erbium Doped Fiber Amplifier (EDFA) are very hot in the optical communication [4-5]. They can amplify the signals in the "all-optical" regime and their performance is independent of the bit rate of the communication systems.

In this section, the amplification mechanisms and the characteristics of the SOA and EDFA are briefly explained. Although they are all-optical amplifiers, they have quite different properties.

3.2.1 The Amplification mechanism of the SOA

Fig. (3.1) shows the structure of the SOA. In fact, it is a laser diode with low reflective coating. Owing to the lack of optical feedback, the laser diode cannot lase itself but it has population inversion. The amplification mechanism of the SOA is similar to the lasing mechanism of the laser diode [4].

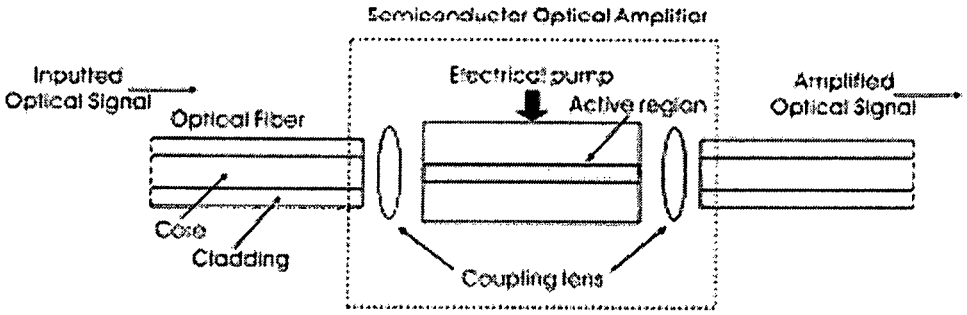

Fig. 3.1 The structure of the SOA

Once the current is injected to the SOA in which electrons gain the energy, they are excited from the ground state to the higher energy state. When the optical signals are introduced to the SOA through coupling devices, the stimulated emission causes electrons to fall into the ground state and simultaneously emits photon with the same wavelength as the incident optical signals. If no optical signal is introduced to the SOA, the electrons will also fall from the higher energy state to the ground state and will emit the photons spontaneously. Such a process forms Amplified Spontaneous Emission (ASE). Fig. (3.2) shows the Two Level System to illustrate the amplification of the SOA.

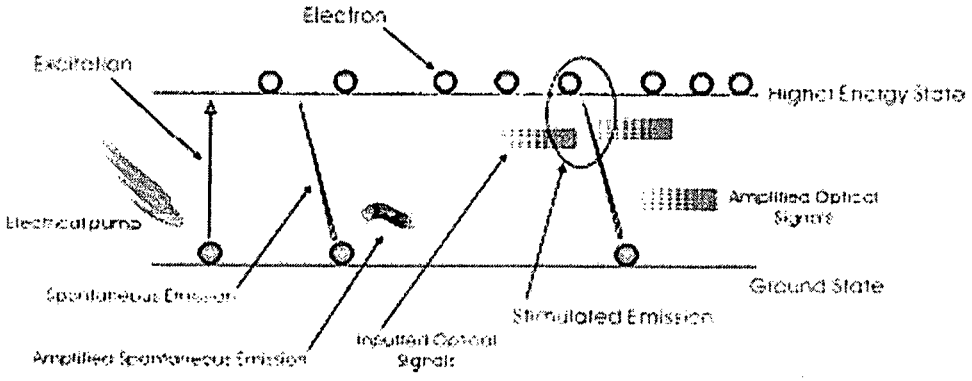

Fig. 3.2 The Two Level System to illustrate the amplification of the SOA

3.2.2 The Amplification mechanism of the EDFA

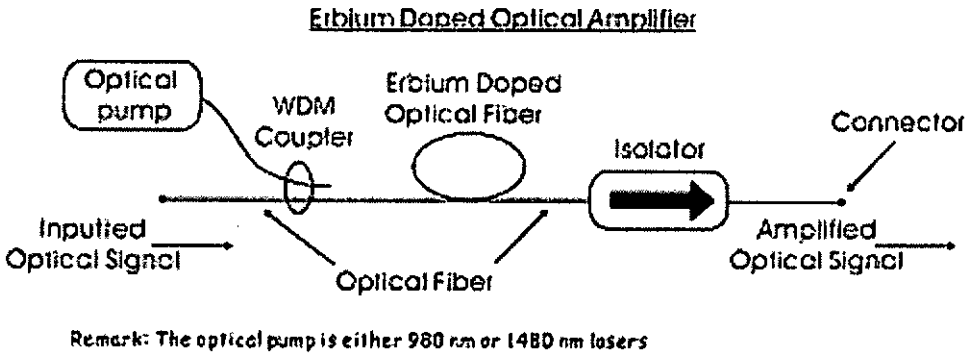

Fig. 3.3 shows the configuration of the EDFA

The EDFA is very common in the optical communication. It includes an isolator, a Wavelength Dependent Multiplexing (WDM) coupler, a 980 nm or 1480 nm optical pump source and a few meters Erbium Doped Optical Fiber, which is shown in Fig. (3.3). In fact, the erbium ions can be excited by lots of wavelengths such as 800 nm, 980 nm, 1480 nm and so on, but only 1480 nm lasers can provide the most efficient optical pump. The EDFA with the 980 nm optical pump can also be found in markets because of its amplification with low noise performance. The impacts of low noise performance on the optical amplifier are very essential in maintaining the SNR of the optical communication system [4-6].

The optical pump can also excite electrons in the erbium ions to the higher energy state in the optical domain so that the population inversion occurs with low noise level. Next, the electrons drop to the metastable state after 1 μs. In the metastable state, the spontaneous emission and stimulated emission occur

simultaneously. If there is not any inputting signal to the EDFA, the electrons will finally drop to the ground state after spontaneous life time (approximate 10 ms). This also causes the ASE in the EDFA. In the stimulated emission, the inputting optical signals to the EDFA triggers the electrons to drop from the metastable state to the ground state and to emit the photons with corresponding wavelengths. However, a little spontaneous emission still occurs. In other words, the ASE can also be found in the spectrum. Fig. (3.4) shows the principles of the spontaneous emission and the stimulated emission in the EDFA [5].

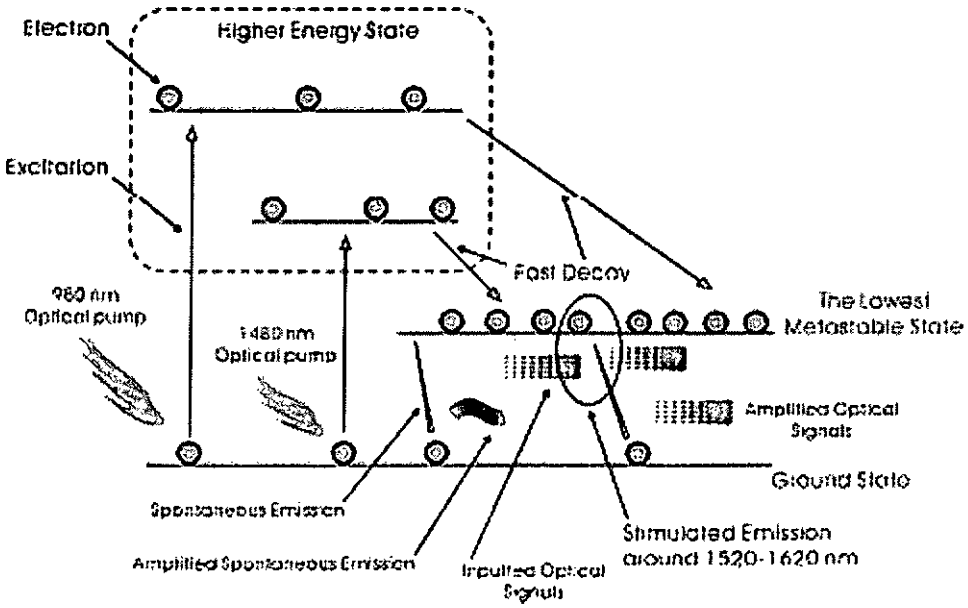

Fig. 3.4 The spontaneous emission and the stimulated emission in the EDFA.

3.2.3 Comparison between the EDFA and the SOA

The significant differences of characteristics between the EDFA and the SOA listed in the Table (3.5) are worthy of attention [4-6]. The gain of the optical amplifiers in their specifications is the small signal gain of the optical amplifiers which is dependent on the pumping power of the amplifiers. The differential gain between orthogonal polarization effects is so small in the EDFA because of a nearly circular waveguide of the Erbium doped optical fiber whereas it is quite large in the SOA owing to the rectangular waveguide of the SOA.

The gain and maximum saturated output power of the EDFA is higher than that of the SOA due to the fact that the pump power of the EDFA is quite larger than that of the SOA.

The noise performance and crosstalk of the SOA are also much serious than that of the EDFA. The Noise Figure in Eq. (3.1) universally quantifies the noise performances of the optical amplifiers [6].

$$\text{Noise Figure}=(\text{SNR})_{in}/(\text{SNR})_{out} \qquad (3.1)$$

Where

$(\text{SNR})_{in}$: the SNR of the input signal of the optical amplifier

$(\text{SNR})_{out}$: the SNR of the output signal of the optical amplifier

The electrical noise is directly introduced to the optical domain via the electrical

pump of the SOA. This causes the poor noise level in the SOA. Due to indirect noise injection from the optical pump of the EDFA driven by electronic circuits, the noise level of the EDFA is typically lower than that of the SOA. Moreover, the nonlinear effects such as Four-Wave Mixing and Cross Gain Saturation can be triggered easily in the SOA by the signal with relatively low optical power. They cause so many adverse effects such as crosstalk between wavelength channels on the optical communication systems.

Features of the optical amplifiers	Long-haul EDFA	SOA
Gain (dB)	>20	10-20
Power (dBm)	>20	10
Noise Figure (dB)	<5	8
Polarization Dependent Gain (dB)	0.1	1
Crosstalk	Low	High
The width of hole burning (nm)	About 11	About 0.6

Table 3.5 The characteristics of the EDFA and the SOA

3.3 The Comb Filter Study

Recently, the Comb filters can be realized by two techniques which are based on

interferometry and diffraction. Various kinds of comb filters such as Fabry-Perot filter with low finesse, Mach-Zehnder filter, Sagnac loop with a Fiber Bragg Grating (FBG), Sampling FBG, Long-Period FBG and so on are proposed for different applications [7-10]. Basically, a comb effect can be realized by the interferometric technique throughout the optical spectrum once the conditions of the interference are satisfied.

3.3.1 Mach-Zehnder Interferometer

In this section, the interference and the Mach-Zehnder Interferometer (MZI) are discussed. A MZI is used together with Erbium Doped Fiber Amplifier (EDFA) in the laser cavity to demonstrate the operation of multi-wavelength laser experimentally.

When wave trains from a coherent light source meet in space, superposition occurs to reinforce and to cancel the wave at the points of space. This causes the interference pattern or fringes.

In order to express the distinctness of the fringes, the quantity called visibility is defined in Eq. (3.2).

$$V = \frac{I_{\max} - I_{\min}}{I_{\max} + I_{\min}} \tag{3.2}$$

Where

I_{max}, I_{min}: The maximum and minimum intensities of the fringes

V: The visibility of the fringes

In order to obtain maximum visibility of the fringes in the interferometer, the coupling ratio of the couplers should equal 0.5.

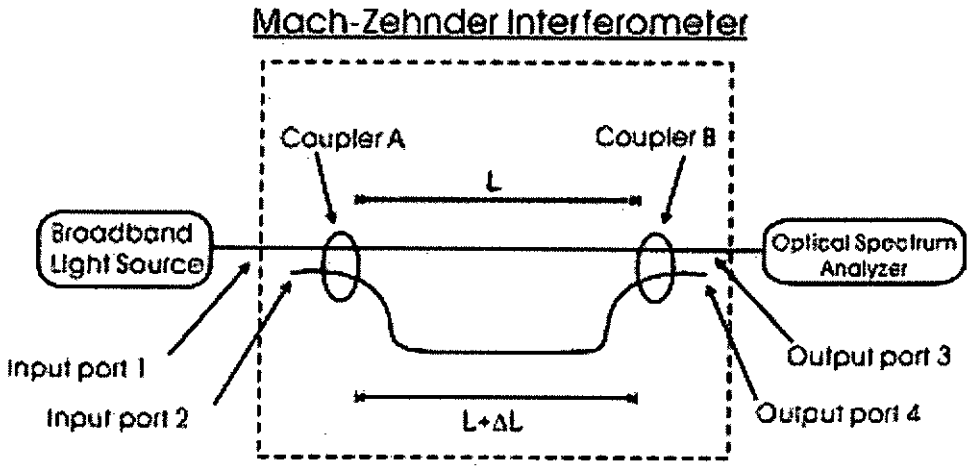

Fig. 3.6 The basic configuration of the Mach-Zehnder interferometer

Fig. (3.6) shows a MZI configuration and its theoretical model is shown in section 3.3.2. The interference output at ports 3 and 4 are complementary [11].

3.3.2 The theoretical model of the Mach-Zehnder interferometer

The transfer functions of the coupler and the OPD are given by

$$M_{coupler}=\begin{bmatrix} \sqrt{k} & i\sqrt{1-k} \\ i\sqrt{1-k} & \sqrt{k} \end{bmatrix} \tag{3.3}$$

$$M_{opd}=\begin{bmatrix} \exp(i\Delta\phi/2) & 0 \\ 0 & \exp(-i\Delta\phi/2) \end{bmatrix} \tag{3.4}$$

Where

k: the ratio of power splitting of the coupler

$\Delta\phi$: the phase difference introduced by the OPD in the interferometer

M: the transfer functions

The transfer functions of the Mach-Zehnder interferometer can be obtained as follow [8]

$$M=\begin{bmatrix} \sqrt{k} & i\sqrt{1-k} \\ i\sqrt{1-k} & \sqrt{k} \end{bmatrix}\begin{bmatrix} \exp(i\Delta\phi/2) & 0 \\ 0 & \exp(-i\Delta\phi/2) \end{bmatrix}\begin{bmatrix} \sqrt{k} & i\sqrt{1-k} \\ i\sqrt{1-k} & \sqrt{k} \end{bmatrix}$$

$$=\begin{bmatrix} (2k-1)\cos(\Delta\phi/2)+i\sin(\Delta\phi/2) & i2\sqrt{k(1-k)}\cos(\Delta\phi/2) \\ i2\sqrt{k(1-k)}\cos(\Delta\phi/2) & (2k-1)\cos(\Delta\phi/2)+i\sin(\Delta\phi/2) \end{bmatrix} \quad (3.5)$$

The relationship between input ports and output ports is given by

$$\begin{bmatrix} E_3 \\ E_4 \end{bmatrix} = M\begin{bmatrix} E_1 \\ E_2 \end{bmatrix} \quad (3.6)$$

If k=0.5,

$$\begin{bmatrix} E_3 \\ E_4 \end{bmatrix} = \begin{bmatrix} i\sin(\Delta\phi/2) & i\cos(\Delta\phi/2) \\ i\cos(\Delta\phi/2) & i\sin(\Delta\phi/2) \end{bmatrix}\begin{bmatrix} E_1 \\ E_2 \end{bmatrix} \quad (3.7)$$

If $E_1 = \sqrt{I_1}\cos(\omega t)$, $E_2 = 0$ is given, the intensities of output ports 3 and 4 will be written as below.

$$E_3 \cdot E_3^* = I_1[1-\cos(\Delta\phi)]/2$$

$$E_4 \cdot E_4^* = I_1[1+\cos(\Delta\phi)]/2 \quad (3.8)$$

Where

I_1: the light intensity in the input port 1

E_3, E_4: the electric field in the output port 3 and 4

Different visibilities of the interference can be observed at ports 3 and 4, if the phase difference between light beams in two arms of the interferometer is changed.

$$\phi = \frac{2\pi n}{\lambda} L \tag{3.9}$$

The phase of the wave is shown in the Eq. (3.9). It depends on the refractive index of the waveguide, the length of the optical path and the wavelength of the light source.

$$\Delta\phi \approx \frac{2\pi n}{\lambda} \Delta L \tag{3.10}$$

Since there is a path difference between two optical paths, an intrinsic phase difference can be found in Eq. (3.10). This induces the interference in the MZI once the coherence length of the light source is larger than the OPD.

$$\frac{d\phi}{d\lambda} = \frac{2\pi n}{\lambda^2} L$$

$$\Delta\phi \approx \frac{2\pi nL}{\lambda^2} \Delta\lambda \tag{3.11}$$

The phase difference can also be varied by the wavelength of the light source in the MZI in the Eq. (3.11). The sinusoidal change of the intensity in the output ports can be observed by linearly changing the phase difference. If the broadband light source is used in the MZI, the comb effect will be observed in the optical spectrum.

Eq. (3.12) shows the overall effect on phase difference by varying the OPD and the wavelength of the light source.

$$\frac{\partial \phi}{\partial L} + \frac{\partial \phi}{\partial \lambda} = (\frac{2\pi n}{\lambda}) + (\frac{2\pi n}{\lambda^2} L)$$

$$\Delta \phi \approx (\frac{2\pi n}{\lambda} \Delta L) + (\frac{2\pi n L}{\lambda^2} \Delta \lambda) \qquad (3.12)$$

3.4 Experiment

In this section, a dual band multi-wavelength erbium-doped fiber laser source formed by cascading two Mach-Zehnder interferometers of different optical path differences in a ring structure is developed. In this system, one of the interferometers selects the operating wavelength region while another acts as a comb filter, and by the use of an optical switch, the simultaneous 10 wavelength lasing around 1555nm region (C-band) or 1565 region (closed to L-band) can be obtained.

3.4.1 Principle of Operation

For a Mach-Zehnder interferometer, the output light intensity can be described as

$$I = \frac{1}{2} I_0 (1 + \cos \frac{2\pi n}{\lambda} \Delta L) \qquad (3.12)$$

Where

I: the output light intensity

I_0: the input light intensity

n: the refractive index of the transmission medium

λ: the wavelength of the light source

ΔL: the optical path difference between the two arms of the interferometer

The phase difference in the Eq. (3.9) is introduced by the interferometer. The transfer function of the interferometer is $(1 + \cos \Delta\phi)/2$, which is a periodic function in the spectral domain, thus the interferometer forms a comb filter.

Erbium-doped fiber possesses a broadband optical gain, when it is used together with a comb filter, a simultaneous multiwavelength laser operation can be obtained. From Eq. (3.10), the laser wavelength spacing is given by

$$\Delta\lambda = \frac{\lambda^2}{n\Delta L} \tag{3.13}$$

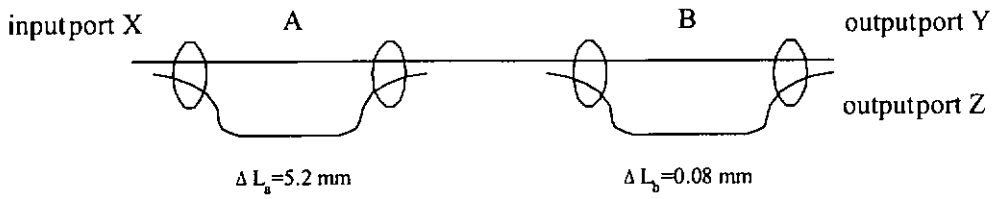

Fig. 3.7 Two Mach-Zehnder interferometers in cascade connection

If two Mach-Zehnder interferometers are in cascade connection in Fig. (3.7), the output light intensity of the system can be expressed as

$$I = \frac{1}{4} I_0 (1 + \cos \frac{2\pi n}{\lambda} \Delta L_a)(1 + \cos \frac{2\pi n}{\lambda} \Delta L_b) \tag{3.14}$$

Where

ΔL_a and ΔL_b: optical path differences of the interferometer A and interferometer B

Once ΔL_a is larger than ΔL_b, $\Delta\lambda_a$ is smaller than $\Delta\lambda_b$. Then, the spectrums of output ports consists of a comb-like curve of period $\Delta\lambda_a$, with its envelop modulated by another slowly varying comb–like curve of period $\Delta\lambda_b$.

The multi-wavelength erbium-doped fiber laser may be obtained by the use of two interferometers in cascade connection, with the laser wavelength spacing defined by $\Delta\lambda_a$, and the whole operating wavelength region determined by $\Delta\lambda_b$.

In Fig. 3.7, the output light intensity in the port Y is complementary to that in the port Z because of the phase difference of π between the two output ports. If an optical switch is used to connect Y and Z alternatively, a dual band multiwavelength erbium-doped fiber laser system can then be built and the lasing wavelengths will be shifted $\Delta\lambda_b/2$ between the two bands.

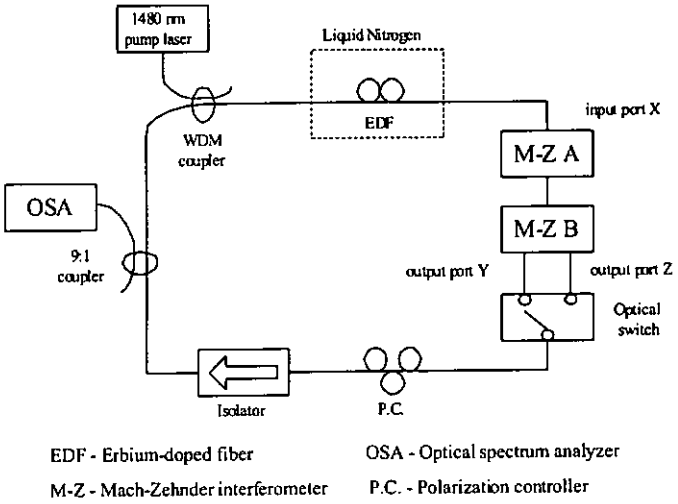

Fig. 3.8 An experimental setup of the dual band multi-wavelength fiber ring laser

The experimental dual band multi-wavelength fiber ring laser system is shown in Fig. 3.8. A 20 meter-long erbium-doped fiber was pumped by a 32 mW laser diode at 1480 nm through a WDM coupler. The erbium-doped fiber had an erbium concentration of 400 ppm and was cooled at 77K with liquid nitrogen to reduce the homogeneous broadening of the fiber laser [12]. Two Mach-Zehnder interferometers, A and B, in a cascade configuration, with ΔL_a = 5.2mm and ΔL_b = 0.08mm respectively, connected to the erbium-doped fiber and an optical switch. A polarization controller was placed in the ring structure to optimize the laser operation and the function of an isolator ensured that the laser was unidirectional. A 90:10 coupler was used to send the laser output to an optical spectrum analyzer with 0.1 nm resolution.

The interferometer A played the role of defining the wavelength spacing of the

multi-wavelength fiber laser source while the interferometer B was used for dual purposes of selecting the lasing wavelength region and stabilizing the laser emission. Although the erbium-doped fiber was cooled by liquid Nitrogen, serious mode competition still existed. The limited bandwidth of the lasing wavelength region restricted the number of the lasing wavelengths and hence a stabilized operation can be obtained.

In the experiment carried out, ΔL_a = 5.2mm and ΔL_b = 0.08mm, the corresponding wavelength spacing were $\Delta\lambda_a \approx 0.5$ nm and $\Delta\lambda_b \approx 20$ nm respectively. A simultaneous 10 wavelengths oscillation with linewidth of 0.15nm, wavelength spacing of 0.5 nm and the bandwidth of the lasing region of 5 nm around 1555 nm (C-band) was obtained and the results are demonstrated in Fig. (3.9). When the interferometer output was switched from port Y to port Z, the lasing region shifted to around 1565 nm (close to L-band) as shown in Fig. (3.10). The amplitude variation between the laser lines was less than 5 dB during the operation and the signal-to-noise ratio obtained was 25 dB.

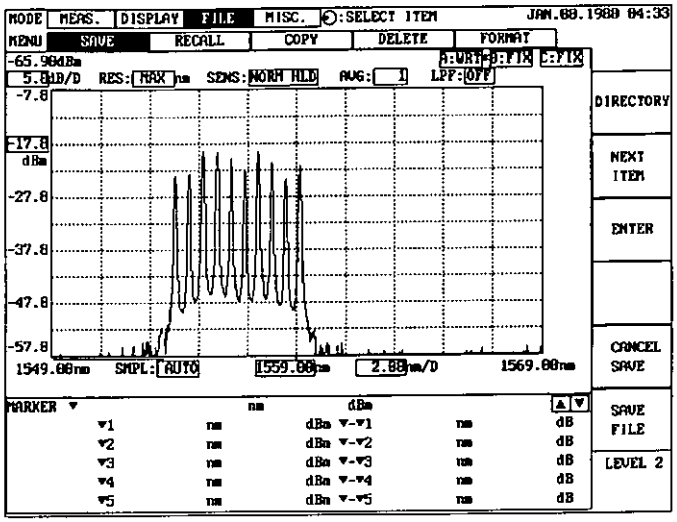

Fig. 3.9 The multi-wavelength laser around 1555 nm

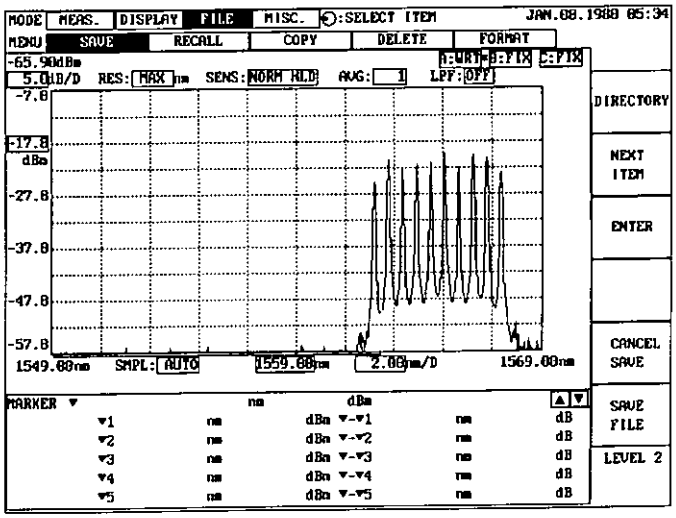

Fig. 3.10 The multi-wavelength laser around 1565 nm

In order to check the stability of the system operation, the laser spectrum was scanned every 1 minute in a consecutive 10 minutes period and the results are shown in Fig. (3.11) and Fig. (3.12).

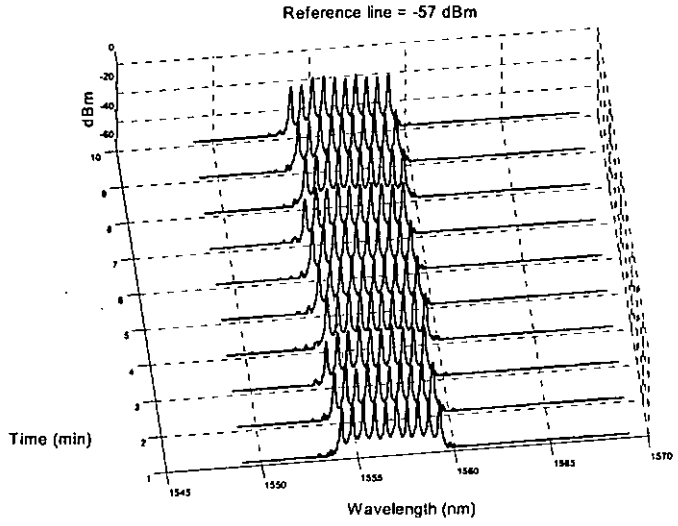

Fig. 3.11 Ten successive scans of the output spectrum around 1555 nm within 10 minutes

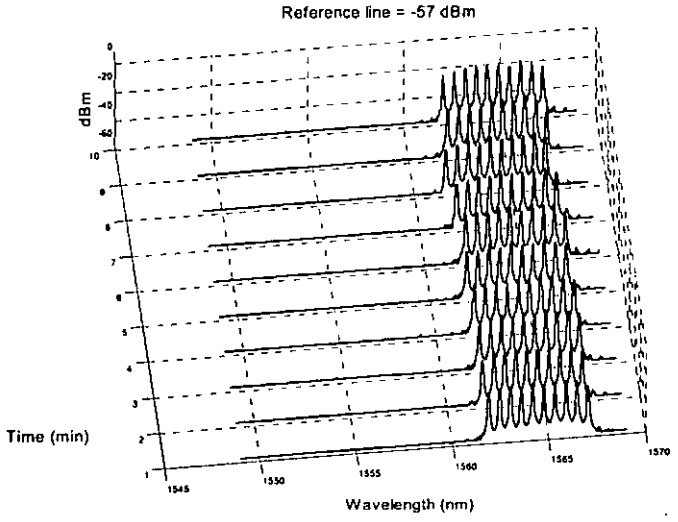

Fig. 3.12 Ten successive scans of the output spectrum around 1565 nm within 10 minutes

The dual band multi-wavelength erbium-doped fiber ring laser system has been demonstrated. The system uses two Mach-Zehnder interferometers in a cascade configuration to enable a simultaneous 10 wavelength lasing operation and dual

wavelength band selection. Such a mechanism increases the system capacity and flexibility. The wavelength spacing is 0.5 nm and the bandwidth of the wavelength region is 20 nm. The amplitude fluctuation between the laser lines is less than 5 dB during the operation and a signal-to-noise ratio better than 25 dB over the whole operating wavelength region has been obtained.

3.5 References

1. M. Zirngibl, "Multifrequency lasers and applications in WDM networks", *IEEE Commun. Magazine*, Vol. 36, No. 12, pp.39-41, Dec. 1998
2. G. Keiser, "Optical Fiber Communications", McGraw-Hill, Boston, 2000
3. S. V. Kartalopoulos, "Introduction to DWDM technology: data in a rainbow", IEEE Press, New York, 2000
4. Mynbaev et al, "Fiber-Optic Communications Technology", Prentice Hall, New Jersey, 1998
5. I. P. Kaminow and T. L. Koch, "Optical Fiber Telecommunications III B", Academic Press, San Diego, 1997
6. D. Derickson, "Fiber Optic Test and Measurement", Prentice Hall, New Jersey, 1998
7. J. Chow, G. Town, B. Eggleton, M. Ibsen, K. Sugden, and I. Bennion, "Multiwavelength generation in an erbium-doped fiber laser using in-fiber comb filters" *IEEE Photon. Technol. Lett.*, vol. 8, No. 1, pp. 60-62, Jan. 1996
8. H. L. An, X. Z. Lin, E.Y.B. Pun, and H. D. Liu, "Multi-wavelength operation of an erbium-doped fiber ring laser using a dual-pass Mach-Zehnder comb filter", *Opt. Comm.*, vol.169, pp.159-165, Oct. 1999
9. X. Shu, S. Jiang, and D. Huang, "Fiber grating sagnac Loop and its

multiwavelength-laser application" *IEEE Photon. Technol. Lett.*, vol. 12, No. 8, pp. 980-982, Aug. 2000

10. J. Sun, Y. Zhang, and X. Zhang, "Multiwavelength lasers based on semiconductor optical amplifiers", *IEEE Photon. Technol. Lett.*, vol. 14, No. 5, pp. 750-752, May 2002

11. E. Hecht, "Optics", Addison-Wesley, New York, 1998

12. S. Yamashita and K. Hotate, "Multiwavelength erbium-doped fibre laser using intracavity etalon and cooled by liquid nitrogen", *Elect. Lett.*, vol. 32, No. 14, pp. 1298-1299, July 1996

Chapter 4

Multi-Wavelength Fiber Ring Laser with A Hybrid Gain Medium

4.1 Background

Multi-wavelength light sources have many applications ranging from Dense Wavelength Division Multiplexing (DWDM) optical fiber communication systems to optical fiber sensor networks [1-2]. Multi-wavelength operation with free of mode competition is always possible when an inhomogeneous gain medium such as a Semiconductor Optical Amplifier (SOA) is used together with wavelength selective elements such as a fiber grating or a comb filter [3-7]. A homogeneous gain medium such as an erbium doped fiber amplifier (EDFA) can be rendered to operate like an inhomogeneous gain medium by cooling the EDFA to liquid nitrogen temperature such that the homogeneous line width is reduced [4-7].

Recently, there have been increased research interests in operation of the multi-wavelength optical fiber laser at room temperature, which may be achieved by introducing a frequency shifter in the laser cavity using an EDFA as the gain medium [8]. The lasing bandwidth and average power of the light source can be increased by the use of a second SOA in the cavity [9]. In order to achieve an uniform and

broadband gain spectrum, the spectral peaks of two chosen SOAs should be sufficiently apart and their corresponding gain profiles should be chosen carefully. Since the semiconductor devices have relatively high noise level, to introduce an extra SOA in the laser cavity will increase the noise. On the other hand, to add an EDFA instead of an SOA into the laser cavity, it may be possible to broaden the gain profile and enhance the gain. It is still not clear under what conditions such a hybrid gain medium can support multi-wavelength operations.

In this Chapter, theoretical analysis for the operation of the multi-wavelength optical fiber laser is carried out. The multi-wavelength operation of a ring laser with a hybrid gain medium constructed by an EDFA and an SOA is experimentally demonstrated. Our analysis shows that multi-wavelength operation can be obtained as long as there is a net gain for the hybrid gain medium.

4.2 Mode Competition

Competition is a common phenomenon in the nature especially in the ecology [10]. Most ecologists are concerned about the population dynamics about two or more species in the same niche. In fact, it is always present in other areas of the science. In order to understand mode competition easily, an ecological example is cited first.

There are two species of fish in a pond. Although they compete for a limited food

supply, they do not prey on another species. Once both species are present in a pond, they will impinge on the available food supply for another species. Thus, the growth rate of the dominant species increases and reaches a saturation point finally. Meanwhile, the dominant species also reduces the growth rate of another species to some extent that it cannot survive in the pond due to lack of food supply. The interaction between the populations of two species can be analyzed by means of a population growth diagram. In the latter part of this chapter, it will be utilized in the analysis of two-mode competition.

The mode competition is one of the laser dynamic behaviors. Most of the laser cavities have a number of potentially oscillating modes. They may lase as the population inversion occurs in the gain medium. The mode competition is commonly observed between simultaneously oscillating modes including longitudinal, transverse and polarization modes. Now, we only discuss the competition in the longitudinal modes as it is concerned with the laser system which we propose. It is basically stemmed from several factors [11].

1. Self-saturation and Cross-saturation effects between modes.

   They are always present in every gain medium although their magnitudes are different.

2. The degree of spectral overlap

It is related to the spacing between two modes.

3. The degree of spatial overlap between modes

   The transverse and longitudinal modes overlap in space. Obviously, this is also related to the polarization of the modes. It is commonly found in the lasers with a Fabry-Perot cavity.

4. Injection locking and frequency pulling effect between modes caused scattering effects or by intra-cavity modulators

   If the laser beam is injected into another laser cavity, it will increase the corresponding photon flux density dramatically. This will affect the mode competition. Such a process is very complicated and is not included in our discussion.

Different modes generally have different gains, losses and saturation coefficients. They will compete for atoms being excited during population inversion in the laser. Oscillation in a single mode will reduce the available gain for the other modes. In some cases, the dominance of one mode leads to the extinction of another mode. This is quite similar to the ecological example which was mentioned before.

In order to illustrate the basic characteristics of the mode competition, the two-mode competition is discussed first. For the sake of simplicity, the back-scattering or cross-scattering effects, which may couple one mode to anothers, are neglected.

The mode competition is solely related to the self-saturation and cross-saturation effects between the two potentially oscillating modes. Although they will be dependent on several factors such as spectral overlap, spatial overlap and so on, which were mentioned before, they also strongly rely on the properties of the gain medium whether it is homogeneous broadening or inhomogeneous broadening. In fact, this is particularly important in analyzing the behavior of the laser system.

In fact, every gain medium should have linear regime and saturated regime respectively. Most Continuous Wave (CW) lasers operate at saturated regime when they reach their steady states. The classical gain model of the lasers with homogeneous broadening is shown in Eq. (4.1).

$$\gamma_m(\omega) = \frac{\gamma_0(\omega)}{1 + \frac{I_\omega}{I_{sat}}} \tag{4.1}$$

Where

$\gamma_0(\omega)$: small signal gain

I_ω, I_{sat} : *output light intensity and saturation light intensity*

Even though this equation can model the gain saturation effect, the cross-saturation effect has not been taken into account. W. Lamb modified this model so as to explain the concepts of the two-mode competition. The modified gain equations are given as follow

The gain equation for mode 1

$$\gamma_1(\omega_1) = \frac{\gamma_{m1}(\omega_1)}{1+\kappa_{11}I_1+\kappa_{12}I_2} \tag{4.2}$$

It can be simplified as

$$\gamma_1(\omega_1) \approx \gamma_{m1}(\omega_1) \times (1-\kappa_{11}I_1-\kappa_{12}I_2) \tag{4.3}$$

The gain equation for mode 2

$$\gamma_2(\omega_2) = \frac{\gamma_{m2}(\omega_2)}{1+\kappa_{21}I_1+\kappa_{22}I_2} \tag{4.4}$$

It can be simplified as

$$\gamma_2(\omega_2) \approx \gamma_{m2}(\omega_2) \times (1-\kappa_{21}I_1-\kappa_{22}I_2) \tag{4.5}$$

Where

I_1, I_2: light intensity of mode 1 and mode 2

$\gamma_{m1}(\omega_1), \gamma_{m2}(\omega_2)$: small signal gain functions of mode 1 and mode 2

κ_{11}, κ_{22}: the self-saturation coefficients of mode1 and mode 2

κ_{12}, κ_{21}: the cross-saturation coefficients of mode1 and mode 2

The approximation of the two gain equations is given in Eq. (4.3) and Eq. (4.5) respectively. This is only valid once the gain medium is not too strongly saturated by the intensity of mode 1 or mode 2. The coefficients of self-saturation and cross-saturation effects are not only inversely proportional to the saturation intensity in the laser medium but also depend on the spatial overlap and spectral overlap.

When two different optical frequencies, whose spatial patterns are identical, are injected into the gain medium with homogeneous broadening, they should have

similar interaction with the gain medium if they are both close to the center of the gain profile. In this case, the coefficients of the self-saturation and cross-saturation effects are almost equal ($\kappa_{11} \approx \kappa_{12} \approx \kappa_{21} \approx \kappa_{22}$).

If the gain medium is inhomogeneous broadening, different spectral packets will be found. In other words, extremely weak cross-saturation effect is present in the gain medium. The coefficient of cross-saturation effect is much smaller than that of the self-saturation effect ($\kappa_{12}, \kappa_{21} << \kappa_{11}, \kappa_{22}$). In modeling such a gain medium, κ_{12}, κ_{21} can be assumed to be zero. Actually, the self-saturation effect is relevant to so called hole burning effect. The depletion of spectral packets in the gain medium is fully dependent on the light intensity of specific optical frequency. If there are two different optical frequencies in the gain medium, two holes will be found in the gain profile. Their depth and width are proportional to the light intensity of the corresponding optical frequency.

4.2.1 The equations about Two-Mode Competition

W. Lamb proposed a set of equations called intensity growth equations [11]. The general equations of two modes are given by

$$\frac{dI_1}{dt} \approx \gamma_{m1} I_1 \times \left(1 - \kappa_{11} I_1 - \kappa_{12} I_2\right) - \gamma_{c1} I_1 \qquad (4.6)$$

$$\frac{dI_1}{dt} \approx (\alpha_1 - \beta_1 I_1 - \theta_{12} I_2) \times I_1 \tag{4.7}$$

$$\frac{dI_2}{dt} \approx \gamma_{m2} I_2 \times (1 - \kappa_{21} I_1 - \kappa_{22} I_2) - \gamma_{c2} I_2 \tag{4.8}$$

$$\frac{dI_2}{dt} \approx (\alpha_2 - \beta_2 I_2 - \theta_{21} I_1) \times I_2 \tag{4.9}$$

Where

γ_{m1}, γ_{m2} : unsaturated growth rates or small signal gain of mode 1 and mode 2

γ_{c1}, γ_{c2} : decay rates in the laser cavity

α_1, α_2: $\gamma_{m1} - \gamma_{c1}, \gamma_{m2} - \gamma_{c2}$

β_1, β_2: $\gamma_{m1}\kappa_{11}, \gamma_{m2}\kappa_{22}$

θ_{12}, θ_{21}: $\gamma_{m1}\kappa_{12}, \gamma_{m2}\kappa_{21}$

The coefficients α_1 and α_2 are obviously the small signal gain minus losses for each mode while the coefficients β_1 and β_2 can still represent the self-saturation and cross-saturation effects. The detailed explanation of steady state solutions is based on Eq. (4.7) and Eq. (4.9)

4.2.2 Steady State Solutions

Once a system reaches the steady state, the rate of change of its variables will tend to be zero. The steady state solutions of mode 1 and mode 2 are given by

$$I_1 = \left(\frac{\alpha_1}{\beta_1}\right) - \left(\frac{\theta_{12}}{\beta_1}\right) I_2 \tag{4.10}$$

$$I_2 = \left(\frac{\alpha_2}{\beta_2}\right) - \left(\frac{\theta_{21}}{\beta_2}\right) I_1 \tag{4.11}$$

There is a linear relationship between the two modes. This can be shown in the plane in Fig. (4.1) which illustrates the interaction between the two modes. Although two lines exist in the plane, we are not sure whether an intersection point exists or not. This is totally dependent on the coefficients in Eq. (4.7) and Eq. (4.9) respectively. In fact, there are two possible cases about intersection in Fig. (4.2). If the two lines do not intersect, there are four intersection points in the plane which are given as follows.

When $I_{2s} = 0$

$$I_{1s} = O_1 = \frac{\alpha_1}{\beta_1} \tag{4.12}$$

$$I_{1s} = T_2 = \frac{\alpha_2}{\theta_{21}} \tag{4.13}$$

When $I_{1s} = 0$

$$I_{2s} = O_2 = \frac{\alpha_2}{\beta_2} \tag{4.14}$$

$$I_{2s} = T_1 = \frac{\alpha_1}{\theta_{12}} \tag{4.15}$$

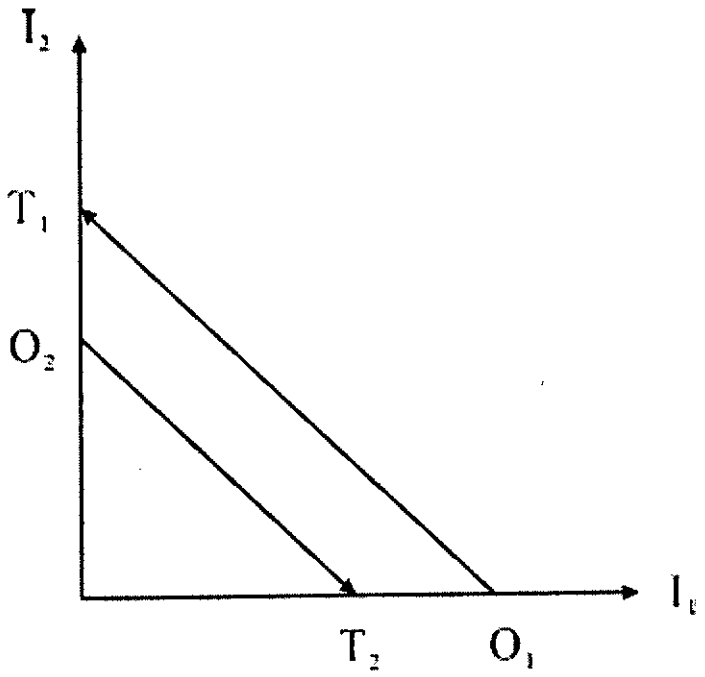

Fig. 4.1 Two lines are in parallel

On the other hand, if the two lines intersect, an extra potential operating point will be found. This may allow two modes to oscillate simultaneously. The analysis of simultaneous two-mode oscillation may be rather complicated than that of single mode oscillation. The general solutions of simultaneous two-mode oscillation are shown as below.

$$I_{1s} = \frac{\alpha_1 - (\theta_{12}/\beta_2)\alpha_2}{(1-C)\beta_1} \tag{4.16}$$

$$I_{2s} = \frac{\alpha_2 - (\theta_{21}/\beta_1)\alpha_1}{(1-C)\beta_2} \tag{4.17}$$

Where

$C = \frac{\theta_{12}\theta_{21}}{\beta_1\beta_2}$: dimensionless coupling factor

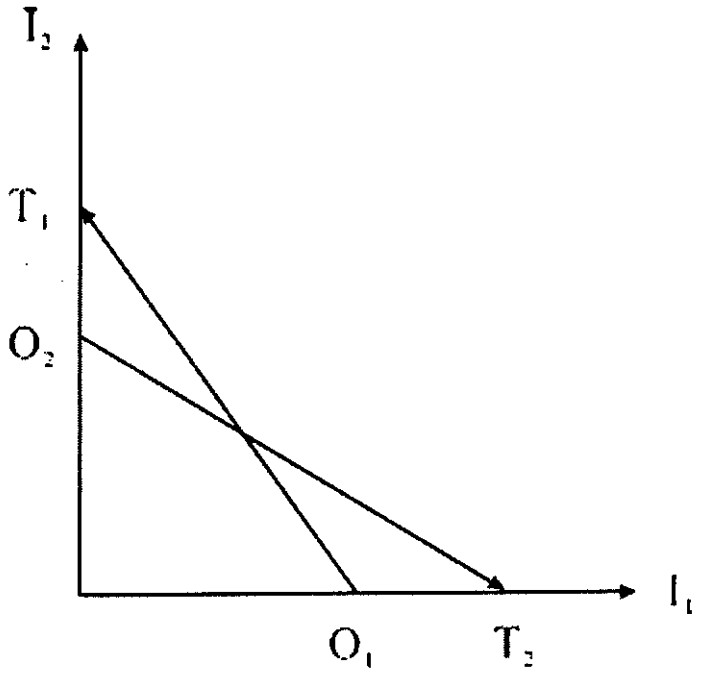

Fig. 4.2 an intersection point is found between two lines

In spite of potential operating points in the plane, only one of them, whose intensity is the strongest, *may survive* in the steady state. Its dominance leads to the extinction of other operating points. In other words, only single operating point actually exists in this case. This can usually be observed in the laser with homogeneous broadening property. A theoretical analysis about this can be done by means of perturbation analysis and linearization.

In order to determine whether the operating point is stable in the steady state or not, all potential operating points should be introduced by small perturbations. As long as the operating points can keep stable under small perturbations, they are stable in the steady state. This can usually be observed in the laser with inhomogeneous

broadening. Therefore, two or more operating points can probably be found in some lasers which have bistable and nonlinear properties. They are not included in our discussion. Actually, the bistability effect is also neglected by the linearization.

4.3 Perturbation Analysis

The Perturbation Analysis (PA), which is one of the standard procedures in the stability analysis, is introduced in this section [12]. Stability problems always appear in various kinds of systems. During an equilibrium state, we need to decide whether the system is stable or not. Theoretically, the system stability can be determined in the equilibrium state by applying small perturbations to the systems. Even though this is always valid in linear systems, most researchers are concerned about its drawbacks in nonlinear systems. Unless assumptions in the PA are made carefully, PA and linearization always fail in the analysis of nonlinear systems. The major reason is that the influence of higher order terms in the linearization is neglected. The conclusion that can be reached by means of approximation may not be in line with the interpretation of the solutions from original equations although the assumptions are made reasonably.

Ordinary Differential Equations (ODE) with respect to time derivatives in Eq. (4.18) govern most mechanical and electrical systems.

$$\frac{dy_1}{dt} = Y_1(y_1,\ldots,y_n,t)$$

...

$$\frac{dy_n}{dt} = Y_n(y_1,...,y_n,t) \tag{4.18}$$

The motion of the above equations is called the unperturbed motion. The analytical solution of ODE can be found. The initial values of the variables $y_1,...,y_n$ are perturbed by small increments $\varepsilon_1,...,\varepsilon_n$ at time $(t = t_0)$. The equations are given as below.

$$y_1 = f_1(t_0) + \varepsilon_1$$

...

$$y_n = f_n(t_0) + \varepsilon_n \tag{4.19}$$

where

f_n: analytical solutions of $\frac{dy_n}{dt}$

ε_n: small increments

Now, $y_n(t)$ called perturbation motion can also be written in Eq. (4.20) in order to ease for further discussion.

$$y_j(t) = f_j(t) + x_j(t), j = 1,2,...,n \tag{4.20}$$

Where

$x_j(t)$: Perturbation functions depend on time

If the absolute values of all $x_j(t)$ are small, the sum of their square will also be small.

$$x_1^2 + x_2^2 + \ldots + x_n^2 = \sum_{j=1}^{n} x_j^2 \tag{4.21}$$

The summation in Eq. (4.21) becomes large when the deviation of at least one variable is large.

Once the equations in such systems satisfy the definition in Eq. (4.22) and Eq. (4.23) proposed by Liapunov, the unperturbed motion is stable [12].

$$\sum_{j=1}^{n} x_{0j}^2 \le \delta \tag{4.22}$$

$$\sum_{j=1}^{n} x_j^2 \le \varepsilon \tag{4.23}$$

Where

$x_{0j}^2 = x_j^2(t_0)$

$x_j^2 = x_j^2(t)$

δ, ε : positive constants ($\delta < \varepsilon$)

This definition can be interpreted as following. The sphere $\sum_{j=1}^{n} x_j^2 = \varepsilon$ with a radius $\sqrt{\varepsilon}$ is considered. If the stable motion starts at any points inside another sphere $\sum_{j=1}^{n} x_{0j}^2 = \delta$ with a radius $\sqrt{\delta}$, it will never go outside the sphere with the radius $\sqrt{\varepsilon}$.

4.3.1 The Equations of perturbed motion

Even though the general solutions of ODE are available, most of the researchers use the stability theory rather than solve the ODEs. By differentiating and expanding Eq. (4.20) into series, we have

$$\frac{dy_j(t)}{dt} = \frac{df_j(t)}{dt} + \frac{dx_j(t)}{dt}$$

$$\frac{dy_j(t)}{dt} = Y_j(y_1,...,y_j,t) + a_{j1}x_1 + a_{j2}x_2 + ... + a_{jn}x_n + X_j^* \tag{4.24}$$

Where

a_{jn}: the coefficients of the series

X_j^*: perturbed terms with higher order

According to Eq. (4.18), the rate of change of perturbed functions with respect to time is given by

$$\frac{dx_j(t)}{dt} \approx a_{j1}x_1 + a_{j2}x_2 + ... + a_{jn}x_n \tag{4.25}$$

Eq. (4.25) is a linearized differential equation when X_j^* is neglected. In many practical cases, the conclusion related to the motions of the systems drawn from the stability analysis is quite useful.

4.4 The Stability in linearization

The stability of the laser system such as mode locked laser can be investigated by means of linearization which may be named as the first order approximation [13-14]. Such a technique is also useful in analyzing nonlinear systems.

Actually, most fundamental equations of lasers are nonlinear ODE. They cannot be solved by the use of analytical methods. The linearization seems to be a relatively simple method in the stability analysis as long as the reasonable assumptions are made carefully. The conclusions obtained from linearized equations are sometimes totally

opposite to that from nonlinear equations which are solved by computational methods. Therefore, essential conditions about linearization should be known as being valid. Once the linearized equations can be formulated, its stability can be determined via the theories proposed by Liapunov and the others.

In general, the linearized equations of the perturbed motion are expressed as

$$\frac{dx_1(t)}{dt} = a_{11}x_1 + a_{12}x_2 + ... + a_{1n}x_n$$

...

$$\frac{dx_j(t)}{dt} = a_{j1}x_1 + a_{j2}x_2 + ... + a_{jn}x_n \tag{4.26}$$

The general solutions of above ODE are given as below

$$x_1 = A_1 e^{\lambda t}$$

...

$$x_n = A_n e^{\lambda t} \tag{4.27}$$

Then,

$$\frac{dx_1}{dt} = \lambda A_1 e^{\lambda t}$$

...

$$\frac{dx_n}{dt} = \lambda A_n e^{\lambda t} \tag{4.28}$$

In steady state, the rate of change of x_n is equal to zero. By substituting Eq. (4.28) into Eq. (4.26), then

$$\begin{bmatrix} a_{11}-\lambda & a_{12} & \cdots & a_{1n} \\ a_{21} & a_{22}-\lambda & \cdots & a_{2n} \\ \cdots & \cdots & \cdots & \cdots \\ a_{n1} & a_{n2} & \cdots & a_{nn}-\lambda \end{bmatrix} \begin{bmatrix} x_1 \\ x_2 \\ \cdots \\ x_n \end{bmatrix} = 0 \qquad (4.29)$$

Because x_n are non-zero, the determinant of the *N*x*N* matrix should be zero in Eq. (4.29). It can be written in terms of λ called the characteristic equation. The stability can be determined according to the theorems (Thm. 4.1-4.5) proposed by Liapunov [12].

Thm. 4.1

If all roots of the characteristics equation have negative real parts, then the unperturbed motion is asymptotically stable.

Thm. 4.2

If at least one of the roots of the characteristic equation has a positive real part, then the unperturbed is unstable.

Thm. 4.3

If some roots of the characteristic equation have zeros as their real part, and the reminder of the roots have negative real parts, then the unperturbed motion is also stable but it is not asymptotically stable.

Thm.4.4 on stability in the first approximation (Liapunov)

If all roots of the characteristic equation of a first approximation have negative real parts, then irrespective of terms of order higher than one, the unperturbed motion is

asymptotically stable.

Thm. 4.5 on instability in the first approximation (Liapunov)

If at least one of the roots of the characteristic equation has a positive real part, then, irrespective of terms of order higher than one, the unperturbed motion is unstable.

4.4.1 The Stability of two-mode competition

The PA has been done in Eq. (4.7) and Eq. (4.9). Even though the roots of the characteristic equation in the system have not been determined, the stability of the laser system can be presented in the plane.

The intensities of mode 1 and 2 in the steady state, which are disturbed by the perturbation terms, are given by

$$I_1(t) = I_{1s} + \varepsilon_1(t) \tag{4.30}$$

$$\varepsilon_1(t) = \varepsilon\phi_1(t)$$

$$I_2(t) = I_{2s} + \varepsilon_2(t) \tag{4.31}$$

$$\varepsilon_2(t) = \varepsilon\phi_2(t)$$

Where

$I_1(t), I_2(t)$: The intensities of mode 1 and 2 under PA

I_{1s}, I_{2s} : The intensities of mode 1 and 2 in the steady state

$\phi_1(t)$, $\phi_2(t)$: The normalized perturbation terms

ε : The coefficient of the small increment

First, we are only concerned about the single mode operation related to the mode 1.

By substituting Eq. (4.30-4.31) into Eq. (4.7), we have

$$\frac{d[I_{1s}+\varepsilon_1(t)]}{dt} \approx \{\alpha_1 - \beta_1[I_{1s}+\varepsilon_1(t)] - \theta_{12}[I_{2s}+\varepsilon_2(t)]\} \times [I_{1s}+\varepsilon_1(t)] \qquad (4.32)$$

By substituting Eq. (4.12) $I_{1s} = O_1 = \frac{\alpha_1}{\beta_1}$ and $I_{2s} = 0$ into Eq. (4.32)

$$\because \frac{dI_{1s}}{dt} = 0 \text{ in the steady state}$$

we have

$$\frac{d\varepsilon_1(t)}{dt} \approx -\alpha_1\varepsilon_1(t) - \frac{\theta_{12}\alpha_1}{\beta_1}\varepsilon_2(t) - \beta_1\varepsilon_1^{\,2}(t) - \theta_{12}\varepsilon_1(t)\varepsilon_2(t) \qquad (4.33)$$

The higher order terms in Eq. (4.33) can be neglected, then

$$\frac{d\varepsilon_1(t)}{dt} \approx -\alpha_1\varepsilon_1(t) - \frac{\theta_{12}\alpha_1}{\beta_1}\varepsilon_2(t) \qquad (4.34)$$

By substituting Eq. (4.30-4.31) into Eq. (4.9), we have

$$\frac{d[I_{2s}+\varepsilon_2(t)]}{dt} \approx \{\alpha_2 - \beta_2[I_{2s}+\varepsilon_2(t)] - \theta_{21}[I_{1s}+\varepsilon_1(t)]\} \times [I_{2s}+\varepsilon_2(t)] \qquad (4.35)$$

By substituting Eq. (4.12) $I_{1s} = O_1 = \frac{\alpha_1}{\beta_1}$ and $I_{2s} = 0$ into Eq. (4.35)

$$\because \frac{dI_{2s}}{dt} = 0 \text{ in the steady state}$$

$$\frac{d\varepsilon_2(t)}{dt} \approx \left\{\alpha_2 - \beta_2\varepsilon_2(t) - \theta_{21}\left[\frac{\alpha_1}{\beta_1} + \varepsilon_1(t)\right]\right\} \times \varepsilon_2(t) \qquad (4.36)$$

The higher order terms in Eq. (4.36) can be neglected, then

$$\frac{d\varepsilon_2(t)}{dt} \approx \left(\alpha_2 - \frac{\alpha_1\theta_{21}}{\beta_1}\right) \times \varepsilon_2(t) \qquad (4.37)$$

Actually, the rate of change of perturbation terms will be negative if the

operating point about single mode operation is stable. Obviously, the rate of change of $\varepsilon_1(t)$ is always negative in Eq. (4.33). In addition, if the rate of change of $\varepsilon_2(t)$ is negative, the condition will be given by

$$\frac{\alpha_1\theta_{21}}{\alpha_2\beta_1} > 1 \quad \text{or}$$
$$\frac{O_1}{T_2} = \frac{\alpha_1/\beta_1}{\alpha_2/\theta_{21}} > 1 \tag{4.38}$$

The single mode operation in mode 1 is similar to that in mode 2. When the mode 2 is dominant in the laser system, its condition is given by

$$\frac{\alpha_2\theta_{12}}{\alpha_1\beta_2} > 1 \quad \text{or}$$
$$\frac{O_2}{T_1} = \frac{\alpha_2/\beta_2}{\alpha_1/\theta_{12}} > 1 \tag{4.39}$$

In order to achieve two modes operation in the laser system, Eq. (4.38) and Eq. (4.39) must be satisfied simultaneously.

$$\frac{O_1}{T_2} \times \frac{O_2}{T_1} = \frac{\theta_{12}\theta_{21}}{\beta_1\beta_2} = C \tag{4.40}$$

where

C: Coupling factor

The two modes operation will be related to weakly coupled oscillator modes if the coupling factor is less than 1 (C<1). On the other hand, the single mode operation will occur as long as the coupling factor is greater than 1 (C>1). This is related to

strongly coupled oscillator modes and serious mode competition. The coupling effects are demonstrated in Fig. (4.3) and Fig. (4.4) respectively.

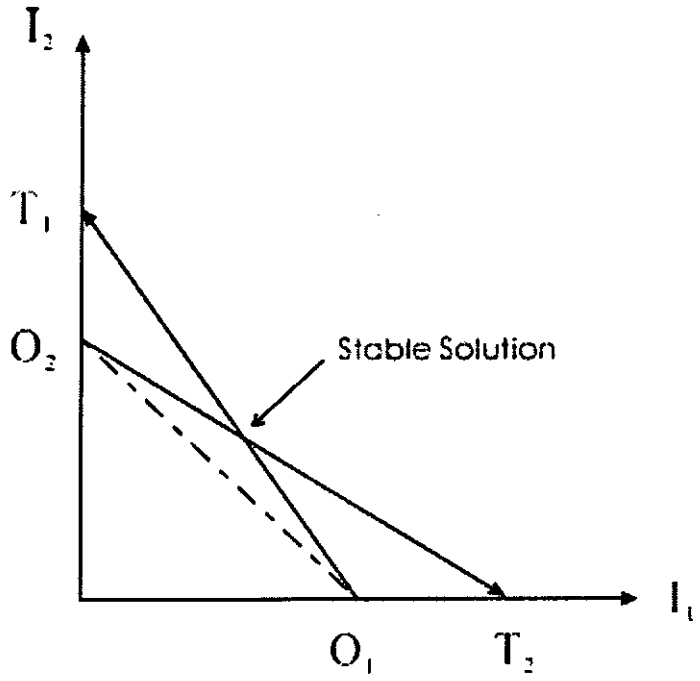

Fig. 4.3 Weakly coupled oscillator modes (C<1)

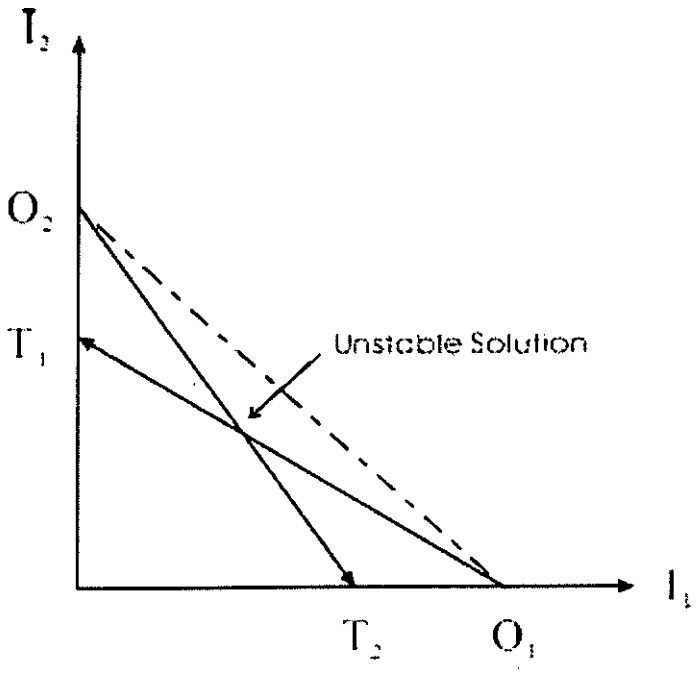

Fig. 4.4 Strongly coupled oscillator modes (C>1)

4.5 Concepts of modeling the laser with a hybrid gain medium

Before the stability of the lasers is studied, they should be modeled to some extent that the effects, which we want to observe, can be included in the model. To date, the laser systems have been studied by means of two opposite approaches. In the first approach, the growth of laser starts from the noise. The entire evolution of light in the cavity is simulated by the use of computational methods. The simulation is usually based on the rate equations. In the second approach, the net change of the intensity during a single pass through the laser cavity is assumed to be zero. This assumption is only valid if the laser system is near equilibrium. A well-known equation based on this assumption, so called the master equation, has been successfully used for modeling the passive mode locking lasers [14].

The modeling of the laser with a hybrid gain medium based on above mentioned assumption is feasible. The minimization of the number of coefficients is necessary in the modeling as a large number of coefficients may cause a too complicated modeling work.

On the one hand, we can observe the inhomogeneous characteristics in the gain medium with homogeneous broadening. On the other hand, the homogeneous properties were also found in the gain medium with inhomogeneous broadening. Normally, we are mainly concerned about the dominant broadening mechanism in the

gain medium.

In order to model the gain medium including both EDFA and SOA in the ring laser operating close to the equilibrium, as shown schematically in Fig. (4.5), the following assumptions are necessarily to be made.

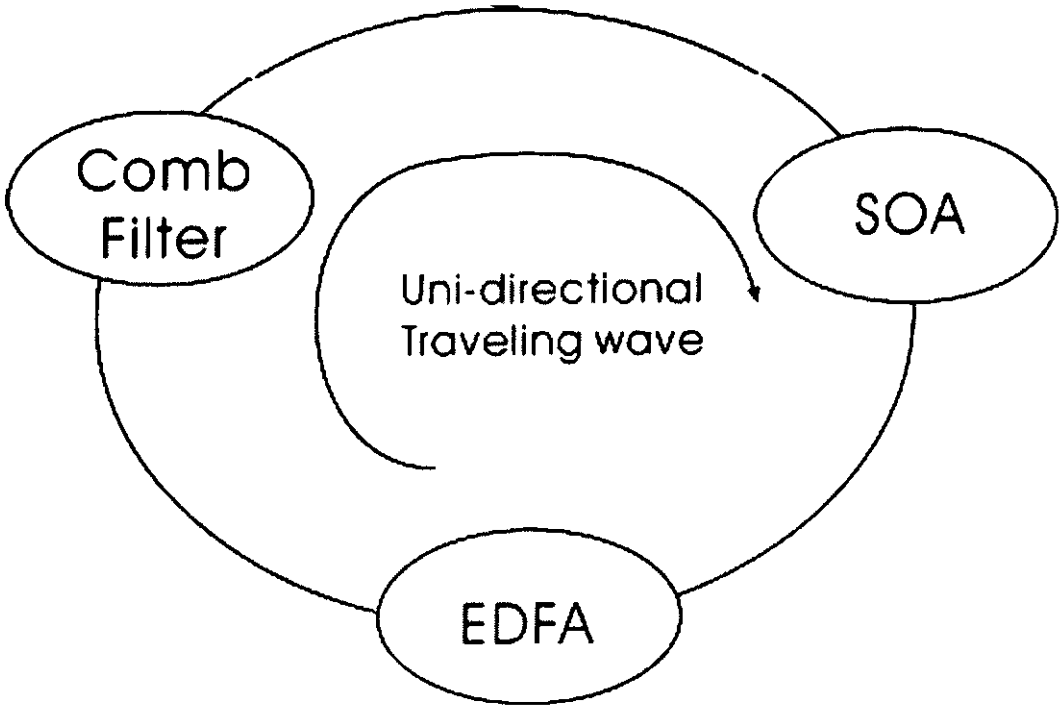

Fig. 4.5 The schematic diagram of the laser with the hybrid gain medium

1. The EDFA and SOA can be assumed as purely homogeneous and inhomogeneous gain medium respectively. Then, the coefficients of self-saturation and cross saturation are nearly the same in the homogeneous gain medium whereas they are extremely different in the inhomogeneous gain medium.
2. The effect of the comb filter can be neglected in the modeling as it only defines the mode spacing in the laser system.

3. In nearly equilibrium state, the intensity changes of various modes during a single pass through the ring cavity are assumed to be very small.

For the sake of brevity, only uni-directional traveling wave is considered. Following above assumptions, Fig. (4.5) can be replaced by Fig. (4.6).

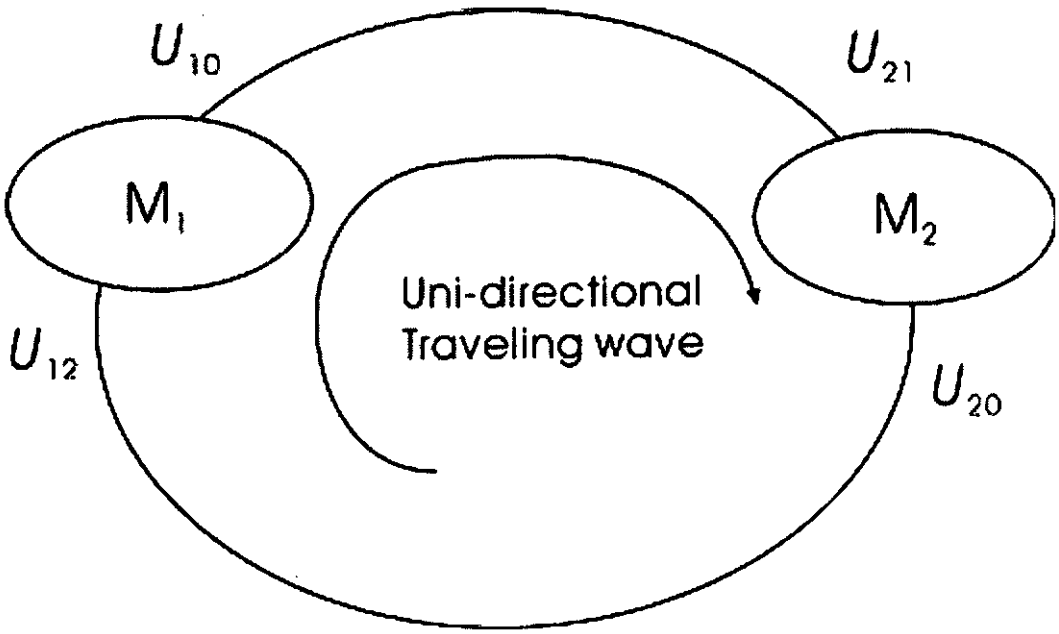

Fig. 4.6 Ring diagram in the modeling

M_1: The equations governing EDFA gain behavior

M_2: The equations governing SOA gain behavior

U_{ij}: the intensity of different modes

In the ring cavity, the relations between the intensities are shown as follows.

$$\because U_{21} = U_{10} \text{ and } U_{12} = U_{20}$$

$$U_{10} = M_1(U_{12})$$

$$U_{20} = M_2(U_{21})$$

$$U_{20} = M_2(M_1(U_{12})) \tag{4.41}$$

4.6 The Stability of N-mode competition in the hybrid gain medium

The competition between N modes will be analyzed by means of PA and linearization again, but modeling of the gain behavior in this section is quite different from that in previous sections. After the number of assumptions have been made, the result in the theoretical analysis shows that N modes become stable once purely homogeneous and inhomogeneous gain media are included in the ring cavity.

According to Lamb's work, self-saturation coefficients are extremely larger than cross-saturation coefficients in the inhomogeneous gain medium ($\kappa_{12}, \kappa_{21} << \kappa_{11}, \kappa_{22}$). However, all coefficients are about the same order of magnitude in the homogeneous gain medium ($\kappa_{11} \approx \kappa_{12} \approx \kappa_{21} \approx \kappa_{22}$) [11]. In a simple analysis, $\beta_n = \kappa_{11}, \kappa_{22}..., \kappa_{nn}, n = 1,2,3...., N$ and $\kappa_{12}, \kappa_{21}, ..., \kappa_{ij} = 0, i \neq j$ are assumed in the model of inhomogeneous gain medium whereas $\kappa = \kappa_{11} \approx \kappa_{12} \approx \kappa_{21} \approx \kappa_{22}...\kappa_{ij}$, (for any i,j) is assumed in the model of homogeneous gain medium. In the simplified ring cavity mentioned in the previous section, the total change of light intensity in the intensity growth equation during each round trip is shown as below.

In a purely inhomogeneous gain medium, the change of light intensity is given by

$$\Delta I_{ei} \approx \left(\alpha_e I_{ei} - \kappa \sum_{j=1}^{N} I_{ei} I_{ej} \right) \Delta t \tag{4.42}$$

In a purely homogeneous gain medium, the change of light intensity is given by

$$\Delta I_{si} \approx \left(\alpha_s I_{si} - \beta I_{si}^2 \right) \Delta t \tag{4.43}$$

The total change of light intensity for each mode during each round trip is given by

$$\Delta I_i = \Delta I_{ei} + \Delta I_{si} \tag{4.44}$$

$$\Delta I_i \approx \left[\left(\alpha_e I_{ei} - \kappa \sum_{j=1}^{N} I_{ei} I_{ej} \right) + \left(\alpha_s I_{si} - \beta I_{si}^2 \right) \right] \Delta t \tag{4.45}$$

When the laser system is near equilibrium, the total change of light intensity is close to zero. Then, $I_i \approx I_j \approx I_{ei} \approx I_{si}, i \neq j$. The system equations for the lasers with the hybrid gain medium can be obtained as follows.

$$\Delta I_i \approx \left[\left(\alpha_e + \alpha_s \right) - \beta I_i - \kappa \sum_{j=1}^{N} I_j \right] I_i \Delta t \tag{4.46}$$

$$\frac{dI_i}{dt} \approx \left(\alpha - \beta I_i \right) I_i - \kappa \sum_{j=1}^{N} I_i I_j, i \neq j \tag{4.47}$$

$$\frac{dI_{is}}{dt} = 0, \left(\alpha - \beta I_i \right) I_i - \kappa \sum_{j=1}^{N} I_i I_j = 0 \tag{4.48}$$

The steady state solutions are given by

$$I_{is} \ldots I_{Ns} = \frac{\alpha}{N\kappa + \beta} \tag{4.49}$$

Where

I_{ei}, I_{si} : The light intensity of every mode in the homogeneous gain medium

I_{si} : The light intensity of every mode in the inhomogeneous gain medium

κ : The cross-saturation coefficients

β : The self-saturation coefficients

α_e : The small signal gain of the homogeneous gain medium

α_s : The small signal gain of the inhomogeneous gain medium

α : The overall gain in the system $(\alpha_e + \alpha_s)$

The steady state solutions are disturbed by small perturbations so as to determine whether they are stable or not.

The perturbation terms is added to the steady state solutions

$$I_i = I_{is} + \varepsilon\phi_i \tag{4.50}$$

The system equation under perturbation is given by

$$\begin{aligned}\frac{dI_i}{dt} &= \alpha(I_{is} + \varepsilon\phi_i) - (\kappa + \beta)(I_{is} + \varepsilon\phi_i)^2 \\ &\quad - \kappa(I_{is} + \varepsilon\phi_i)\sum_{j=1}^{N}(I_{js} + \varepsilon\phi_{js}), i \neq j\end{aligned} \tag{4.51}$$

The linearization is made in Eq. (4.51) so as to determine whether the system is stable or not near the equilibrium.

$$\frac{d\phi_i}{dt} = [\alpha - ((N+1)\kappa + 2\beta)I_{is}]\phi_i - \kappa I_{is}\sum_{j=1}^{N}\phi_j, i \neq j \tag{4.52}$$

The perturbation terms are supposed to be $\phi_i = e^{\lambda t}$, as the exponential growth and decay rate can show the system stability. Then, the system equation can be written as:

$$\begin{bmatrix} \alpha-((N+1)\kappa+2\beta)I_{1s}-\lambda & -\kappa I_{1s} & \cdots & -\kappa I_{1s} \\ -\kappa I_{2s} & \alpha-((N+1)\kappa+2\beta)I_{2s}-\lambda & \cdots & \cdots \\ \cdots & \cdots & \cdots & \cdots \\ -\kappa I_{Ns} & \cdots & \cdots & \alpha-((N+1)\kappa+2\beta)I_{Ns}-\lambda \end{bmatrix} \begin{bmatrix} \phi_1 \\ \phi_2 \\ \cdots \\ \phi_N \end{bmatrix} = 0 \tag{4.53}$$

The determinant of NxN matrix in Eq. (4.53) should be zero if the perturbation terms are non-zero elements.

$$\begin{vmatrix} \frac{-\alpha(\kappa+\beta)}{N\kappa+\beta}-\lambda & \frac{-\alpha\kappa}{N\kappa+\beta} & \cdots & \frac{-\alpha\kappa}{N\kappa+\beta} \\ \frac{-\alpha\kappa}{N\kappa+\beta} & \frac{-\alpha(\kappa+\beta)}{N\kappa+\beta}-\lambda & \cdots & \frac{-\alpha\kappa}{N\kappa+\beta} \\ \cdots & \cdots & \cdots & \cdots \\ \frac{-\alpha\kappa}{N\kappa+\beta} & \cdots & \cdots & \frac{-\alpha(\kappa+\beta)}{N\kappa+\beta}-\lambda \end{vmatrix} = 0 \tag{4.54}$$

$$\begin{vmatrix} \frac{-N\alpha\kappa}{N\kappa+\beta}-\frac{\alpha\beta}{N\kappa+\beta}-\lambda & \frac{-N\alpha\kappa}{N\kappa+\beta}-\frac{\alpha\beta}{N\kappa+\beta}-\lambda & \cdots & \frac{-N\alpha\kappa}{N\kappa+\beta}-\frac{\alpha\beta}{N\kappa+\beta}-\lambda \\ \frac{-\alpha\kappa}{N\kappa+\beta} & \frac{-\alpha(\kappa+\beta)}{N\kappa+\beta}-\lambda & \cdots & \frac{-\alpha\kappa}{N\kappa+\beta} \\ \cdots & \cdots & \cdots & \cdots \\ \frac{-\alpha\kappa}{N\kappa+\beta} & \cdots & \cdots & \frac{-\alpha(\kappa+\beta)}{N\kappa+\beta}-\lambda \end{vmatrix} = 0$$

$$(-\alpha-\lambda)\frac{N\kappa+\beta}{-\alpha\kappa}\begin{vmatrix} \frac{-\alpha\kappa}{N\kappa+\beta} & \frac{-\alpha\kappa}{N\kappa+\beta} & \cdots & \frac{-\alpha\kappa}{N\kappa+\beta} \\ \frac{-\alpha\kappa}{N\kappa+\beta} & \frac{-\alpha(\kappa+\beta)}{N\kappa+\beta}-\lambda & \cdots & \frac{-\alpha\kappa}{N\kappa+\beta} \\ \cdots & \cdots & \cdots & \cdots \\ \frac{-\alpha\kappa}{N\kappa+\beta} & \cdots & \cdots & \frac{-\alpha(\kappa+\beta)}{N\kappa+\beta}-\lambda \end{vmatrix} = 0$$

$$(-\alpha-\lambda)\frac{N\kappa+\beta}{-\alpha\kappa}\begin{vmatrix} \frac{-\alpha\kappa}{N\kappa+\beta} & \frac{-\alpha\kappa}{N\kappa+\beta} & \cdots & \frac{-\alpha\kappa}{N\kappa+\beta} \\ 0 & \frac{-\alpha\beta}{N\kappa+\beta}-\lambda & \cdots & 0 \\ \cdots & \cdots & \cdots & \cdots \\ 0 & \cdots & \cdots & \frac{-\alpha\beta}{N\kappa+\beta}-\lambda \end{vmatrix} = 0$$

The characteristic equation of the laser system is given by

$$\left(\frac{-\alpha\beta}{N\kappa+\beta}-\lambda\right)^{N-1}(-\alpha-\lambda)=0 \tag{4.55}$$

Linear stability analysis shows that the roots of the characteristic polynomial for the N wavelengths are $-\alpha$ and $-\beta\alpha/(N\kappa+\beta)$ with the second solution $(N-1)$ degenerate. Thus a ring laser with both EDFA and SOA used as the gain medium can support

multi-wavelength operation as long as the net gain α is larger than zero.

It can be observed that there are only a number of independent ODEs in the model of purely inhomogeneous gain medium in which the general solution of each mode can be found. In other words, the multi-wavelength generation can be obtained in purely inhomogeneous gain medium.

4.7 Experiment

In order to further understand the interaction between the homogeneous and inhomogeneous gain medium, the experiment to compare the hybrid gain medium with the inhomogeneous gain medium alone in the ring cavity has been conducted. The benefits offered by the hybrid gain medium can be confirmed by the experiment.

The EDFA and SOA are typically homogeneous and inhomogeneous gain medium respectively. The widths of hole burning of the EDFA and SOA are 11 nm and 0.6 nm respectively [15-16]. In this experiment, an EDFA and an SOA are used together in a ring laser cavity to form a hybrid gain medium.

The experimental setup was shown in Fig. (4.7). The C-band EDFA consisted of a 7-meter section of erbium-doped fiber with an erbium concentration of 400 ppm. The EDFA was pumped by a 980 nm laser diode with the pumping optical power of 25 mW. The SOA was driven by a 120 mA current source. The Mach-Zehnder

interferometer acted as a comb filter with 0.5 nm Free Spectral Range (FSR). A polarization controller was placed within the fiber ring to optimize the laser operation and an isolator was used to ensure unidirectional lasing. An optical spectrum analyzer with 0.1 nm resolution was used to monitor the lasing spectrum via a 9:1 fiber coupler at room temperature. Fig. (4.8) shows the results recorded by OSA for 10 successive scans within 10 minutes. Twenty-two wavelengths with SNR of 25 dB were observed within 3 dB bandwidth. The fluctuation of the peak intensity at 1564.88 nm was measured to be +/- 0.65 dB.

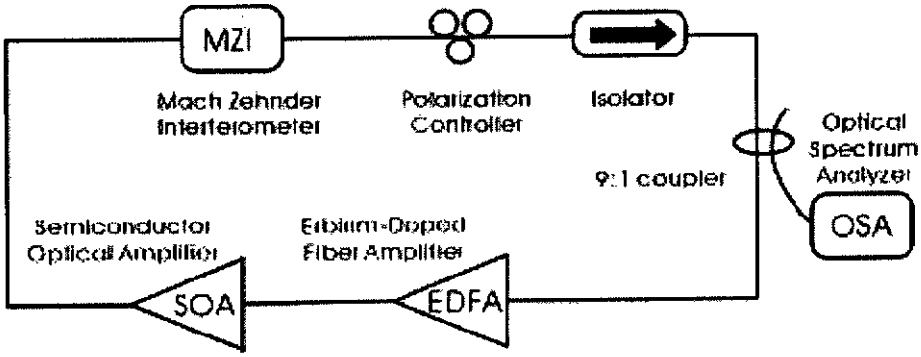

Fig. 4.7 Experiment Setup

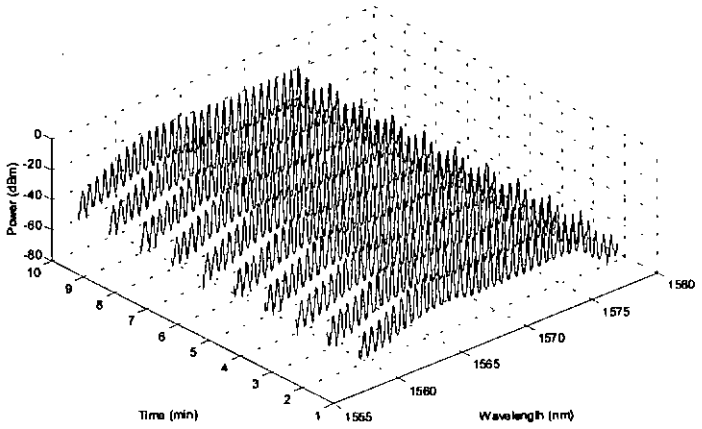

Fig. 4.8 Ten successive scans of the output spectrum within 10 minutes

In theoretical analysis, we show that the overall gain in the ring cavity plays an important role in the stability of *N*-mode competition. The laser system with such a hybrid gain medium is always stable in the multi-wavelength generation provided that the overall gain is positive, i.e. the small signal gains are greater than the loss in the ring cavity. The pumping current to the SOA and pumping optical power to the EDFA also change the overall gain in the ring cavity. Actually, the hybrid gain medium is either biased toward the homogeneous broadening or toward inhomogeneous broadening by means of changing the ratio of the small signal gain of the EDFA and SOA.

By changing pumping currents to the SOA and pumping optical power to the EDFA respectively, Fig. (4.9) - Fig. (4.15) shows different laser spectra.

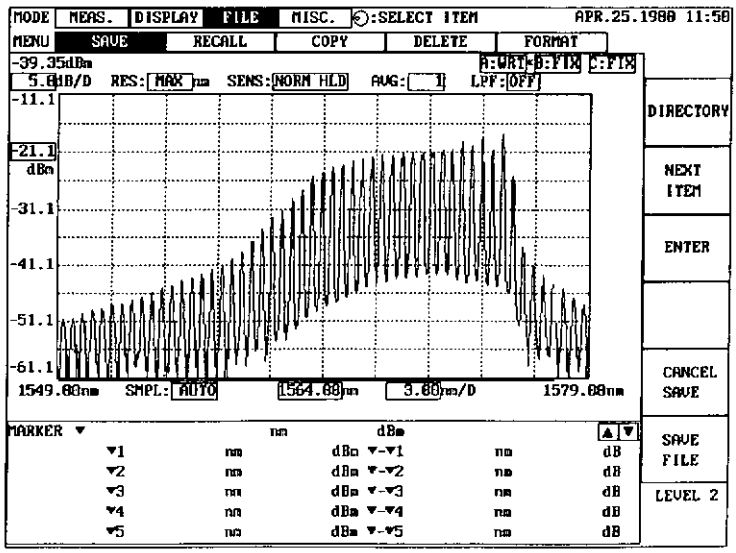

Fig. 4.9 In the ring cavity, only SOA is driven by the 120 mA current source.

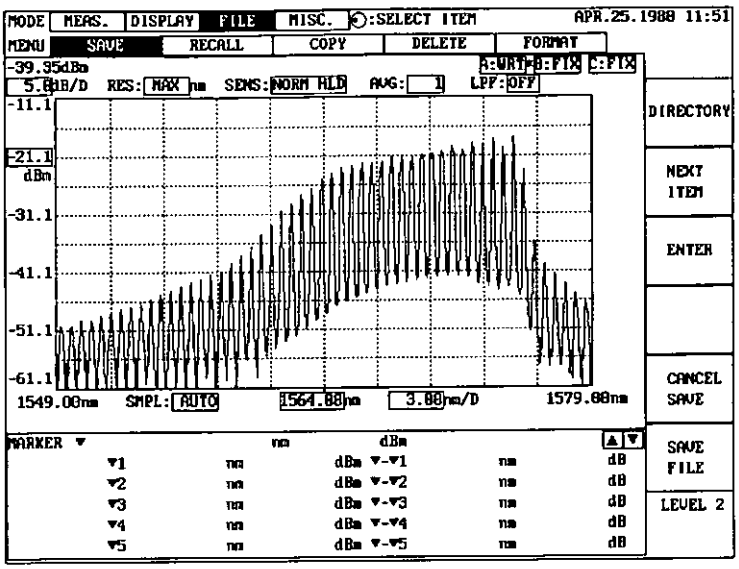

Fig. 4.10 In the ring cavity, only SOA is driven by the 140 mA current source.

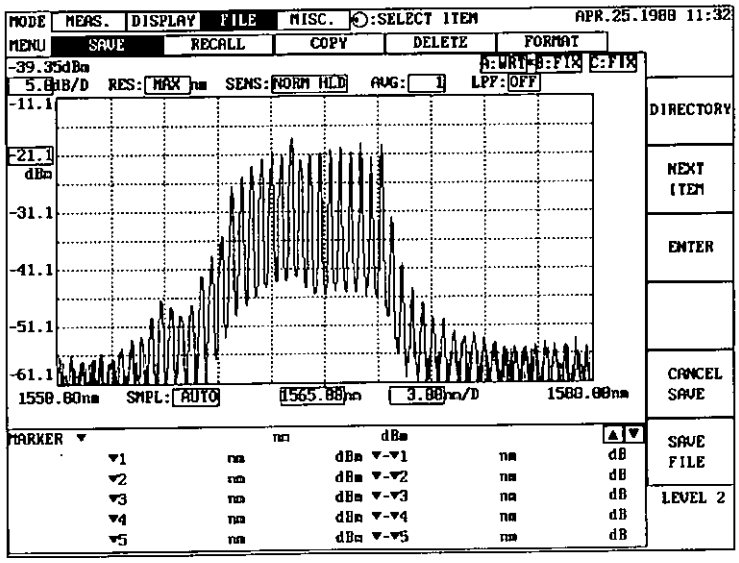

Fig. 4.11 In the ring cavity, the EDFA is pumped by the 62 mW optical pump and the SOA is driven by the 90 mA current source.

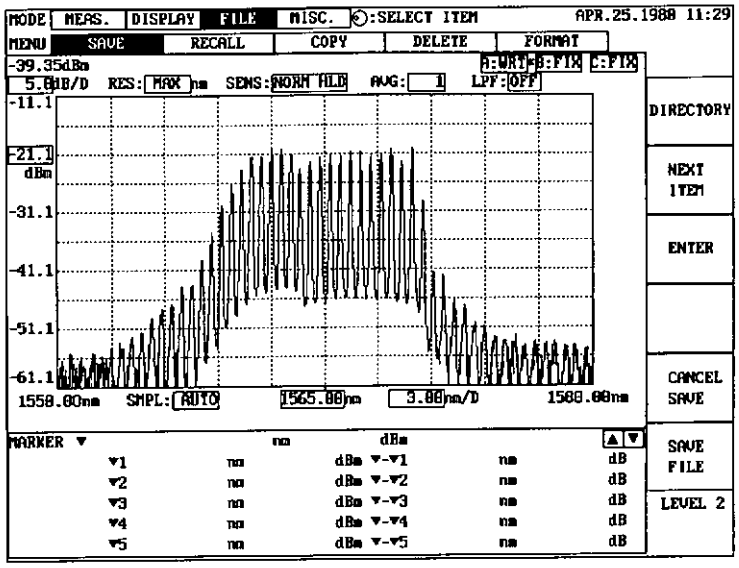

Fig. 4.12 In the ring cavity, the EDFA is pumped by the 38 mW optical pump and the SOA is driven by the 90 mA current source.

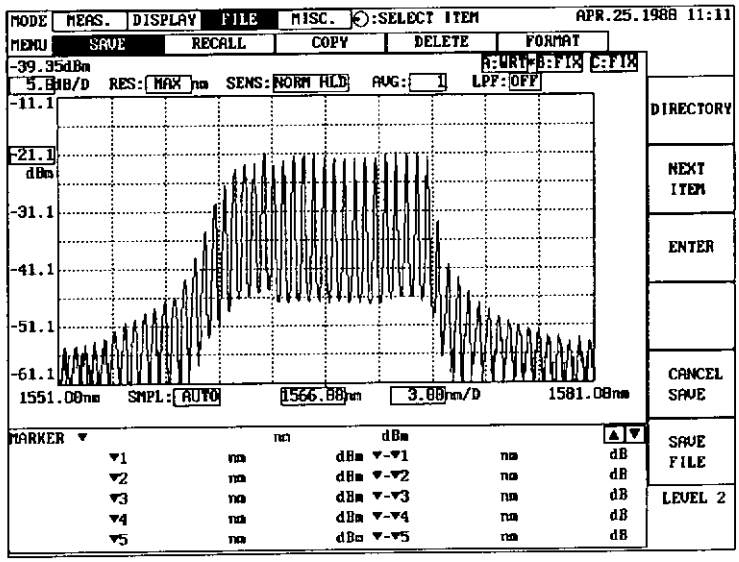

Fig. 4.13 In the ring cavity, the EDFA is pumped by the 20 mW optical pump and the SOA is driven by the 90 mA current source.

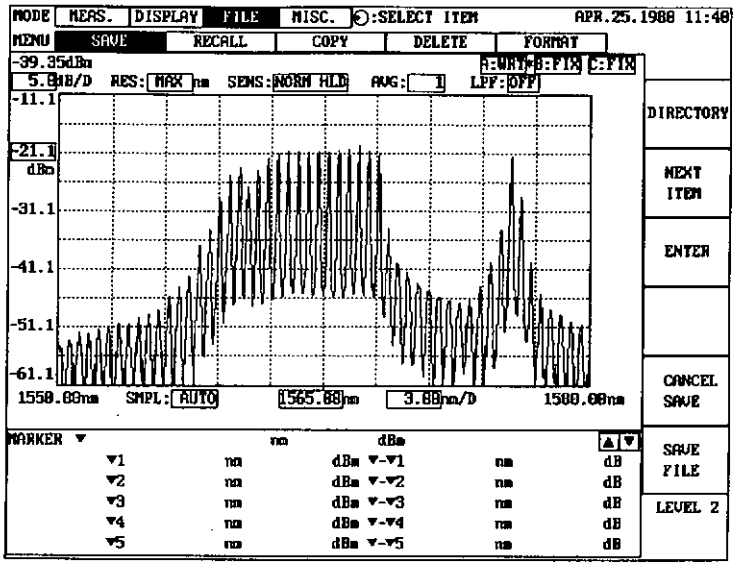

Fig. 4.14 In the ring cavity, the EDFA is pumped by the 13 mW optical pump and the SOA is driven by the 90 mA current source.

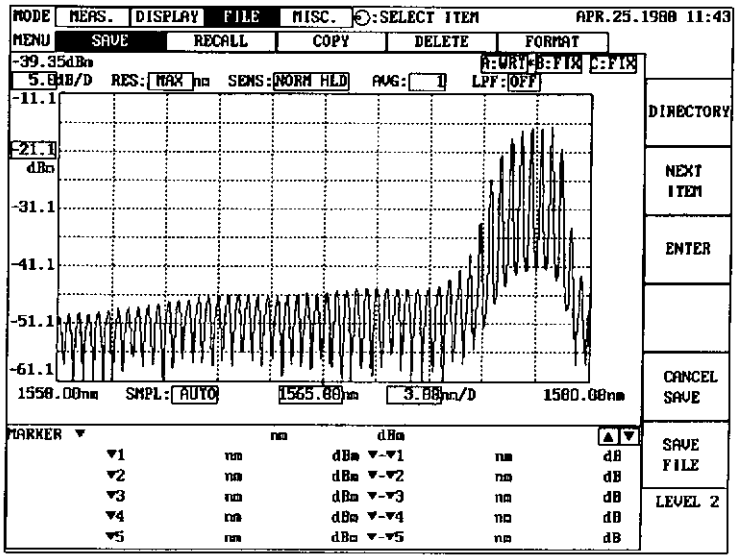

Fig. 4.15 In the ring cavity, the EDFA is pumped by the 5 mW optical pump and the SOA is driven by the 90 mA current source.

The laser spectra with only SOA used as the gain medium are demonstrated in Fig. (4.9) and Fig. (4.10), corresponding to 120 mA and 140 mA pumping currents respectively. Fig. 4.9 shows a simultaneous lasing of 14 wavelengths within a 3 dB

bandwidth with oscillation bandwidth of 8 nm and SNR of 23 dB. The lasing operation with oscillation bandwidth of 9 nm and SNR of 22 dB is shown in Fig. (4.10).

Fig. (4.11) shows the multi-wavelength laser operation when the pumping optical power of the EDFA is 62 mW and the pumping current of the SOA is 90 mA. Its oscillation bandwidth and average SNR are 7.5 nm and 23 dB respectively. In order to investigate the interaction between the pumping power and lasing action, only pumping optical power of the EDFA decreases while that of the SOA remain unchanged at 90 mA in the hybrid gain medium. While the pumping optical power of the EDFA decreases from 62 mW to 38 mW, the oscillation bandwidth increases to 9 nm, as shown in Fig. (4.12). If the pumping optical power further decreases to 20 mW, the oscillation bandwidth increases to 11 nm, as shown in Fig. (4.13). The average SNR of the lasing actions in Fig. (4.11-4.13) are about 25 dB.

The oscillation bandwidth of the multi-wavelength laser in Fig. (4.14) is 7 nm as the pumping optical power of the EDFA decreases to 13 mW. When it is adjusted to be 5 mW, the laser operations cannot be observed around 1565 nm as shown in Fig. (4.15). The loss becomes larger than the gain in the laser cavity, as an Erbium Doped Fiber (EDF) acts as an absorber when the pumping optical power is low. However, several wavelengths still lase around 1577 nm in Fig. (4.15), as the absorption of EDF

around 1577 nm is low and the gain from the SOA is still available. It has been found in the experiment that the oscillation bandwidth and the number of wavelengths will decrease once the pumping optical power of the EDFA in the hybrid gain medium increase.

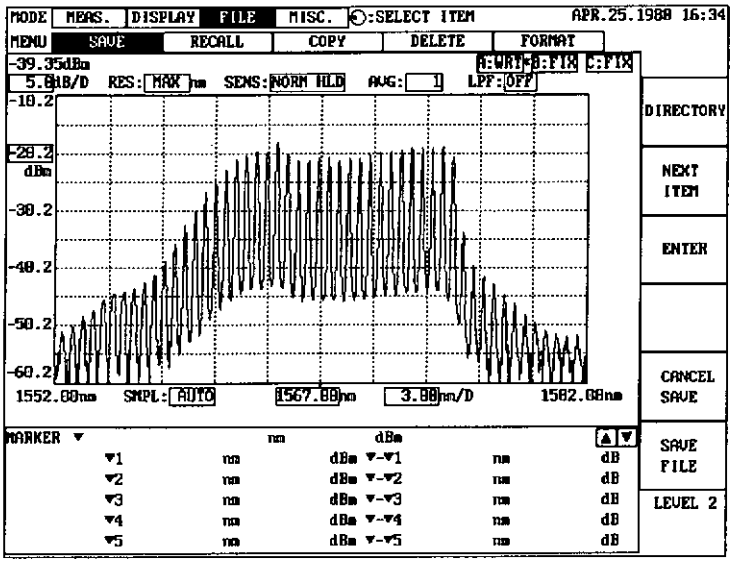

Fig. 4.16 An optimized output spectrum is obtained. In the ring cavity, the EDFA is pumped by the 27 mW optical pump and the SOA is driven by the 120 mA current source.

After optimizing the laser operations, the system output is demonstrated in Fig. (4.16) in which 22 lasing wavelengths with SNR of 25 dB are observed within a 3 dB bandwidth. Fig. (4.8) shows the output recorded by an optical spectrum analyzer for 10 successive scans within 10 minutes.

In order to further investigate the stability of the lasing wavelengths, a stable Fabry-Perot filter may be used to filter out one of the wavelengths whose optical power is subsequently converted to electrical power by a photodetector. Then, an

oscilloscope can continuously monitor the electrical power. In addition, one of the lasing wavelengths can also be modulated by signals with random bit patterns in a Bit Error Rate Test. By observing the eye diagram, the stability of the laser can be determined.

We also conduct an experiment with only the SOA in the ring cavity (The EDFA shown in Fig. (4.7) is removed). Fig. (4.9) shows a simultaneous lasing of 14 wavelengths with SNR of 23 dB within a 3 dB bandwidth. The SNR of the laser with SOA alone is 2-3 dB lower than that with hybrid gain medium. This may be caused by the poor noise performance of the SOA. Moreover, the number of wavelengths from the laser with SOA alone is considerably smaller than that from the laser system with hybrid gain medium. It is expected that using an L-band EDFA together with the SOA will broaden the lasing bandwidth and will increase the number of wavelengths in the ring laser.

4.8 Summary of this experiment

The laser with the hybrid gain system using an EDFA and a SOA was demonstrated to support multi-wavelength operation at room temperature. The stable operation of 22 wavelengths within 3 dB bandwidth was achieved and the SNR of 25 dB was obtained. The hybrid system suppresses the mode competition from the laser

system with EDFA alone while reduces relatively large amplified spontaneous emission (ASE) noise in the system with only SOA. In order to compare the performances of the hybrid gain medium with that of the SOA, the two overall gains should be about same. Actually, the laser with the hybrid gain medium may be compared with the laser associated with two SOAs. Since the noise figure of EDFA is much lower than that of SOA, the noise performance of the hybrid gain laser becomes much lower than that of the laser associated with two SOAs. Replacing the C-band EDFA with a L-band EDFA is expected to further broaden the lasing bandwidth and to increase the number of wavelengths in the ring laser.

4.9 References

1. R. Monnard, A.K. Srivastava, C.R. Doerr et al, "16-channel 50 GHz channel spacing long-haul transmitter for DWDM systems", *Elect. Lett.*, vol. 34, No. 8, pp. 765-766, April 1998

2. L. Talaverano, S. Abad, S. Jarabo and M. López-Amo, "Multiwavelength fiber laser sources with Bragg-grating sensors multiplexing capability", *J. Lightwav. Technol.* Vol. 19, No. 4, pp. 553-558, April 2001

3. J. Sun, Y. Zhang, and X. Zhang, "Multiwavelength lasers based on semiconductor optical amplifiers", *IEEE Photon. Technol. Lett.*, vol. 14, No. 5, pp. 750-752, May 2002

4. J. Chow, G. Town, B. Eggleton, M. Ibsen, K. Sugden, and I. Bennion, "Multiwavelength generation in an erbium-doped fiber laser using in-fiber comb filters" *IEEE Photon. Technol. Lett.*, vol. 8, No. 1, pp. 60-62, Jan. 1996

5. X. Shu, S. Jiang, and D. Huang, "Fiber grating sagnac Loop and its multiwavelength-laser application" *IEEE Photon. Technol. Lett.*, vol. 12, No. 8, pp. 980-982, Aug. 2000

6. S. Yamashita and T. Baba, "Spacing-tunable multiwavelength fibre laser", *Elect. Lett.*, vol. 37, No. 16, pp. 1015-1017, Aug. 2001

7. S. Yamashita and K. Hotate, "Multiwavelength erbium-doped fibre lasr using

intracavity etalon and cooled by liquid nitrogen", *Elect. Lett.*, vol. 32, No. 14, pp. 1298-1299, July 1996

8. A. Bellemare, et al, "Room temperature multifrequency erbium-doped fiber lasers anchored on the ITU frequency grid", *J. Lightwav. Technol.*, Vol. 18, No. 6, pp. 825-831, June 2000

9. N. Pleros, C. Bintjas, M. Kalyvas, et al, "Multiwavelength and power equalized SOA laser sources", *IEEE Photon. Technol. Lett.*, vol. 14, No. 5, pp. 693-695, May 2002

10. William E. Boyce and Richard C. DiPrima, "Elementary differential equations and boundary value problems", John Wiley & Sons, Inc., Sixth edition, pp. 459-512, 1997

11. A.E. Siegman, "Lasers", University Science Books, 1986, pp. 992-999

12. David R. Merkin, "Introduction to the theory of stability", Springer-Verlag, 1997

13. C.J. Chen, P.K.A. Wai and C.R. Menyuk, "Stability of passively mode-locked fiber lasers with fast saturable absorption", *Optics Lett.*, Vol. 19, pp. 198-200, 1994

14. H.A. Haus, J.G. Fujimoto and E.P. Ippen, "Structures for additive pulse mode locking", *J. Opt. Soc. Am. B*, Vol. 8, No. 10, pp. 2068-2076, 1991

15. E. Desurvire, J.L. Zysking and J.R. Simpson, "Spectral gain hole-burning at

1.53 μm in erbium-doped fiber amplifiers", *IEEE Photon. Technol. Lett.*, vol. 2, No. 4, pp. 246-248, April 1990

16. B. Yu, D.H. Kim and B. Lee, "Multiwavelength pulse generation in semiconductor-fiber ring laser using a sampled fiber grating", *Optics Comm.*, vol. 200, pp. 343-347, Dec. 2001

Chapter 5

Conclusion and Further Work

5.1 Conclusion

The study of the multi-wavelength fiber ring laser is divided into two parts in this thesis; comb filter and gain medium. The comb filter can ensure the wavelength spacing of the laser output. The gain medium provides the power gain to different lasing wavelengths in order to compensate the loss in the laser cavity.

In fact, the interferometers and Sampled Fiber Bragg Grating can be used to realize the comb effect. In this work, two Mach-Zehnder interferometers with different optical path difference were cascaded in an Erbium Doped Fiber (EDF) ring laser at the temperature of liquid Nitrogen (77K), which can reduce homogeneous linewidth of EDF so as to avoid the mode competition in the multi-wavelength operation. One of the interferometers can act as the comb filter while another is an interleaver for selecting lasing centers. By the use of an optical switch, simultaneous ten wavelength lasers around 1555 nm or around 1565 nm were obtained.

The laser with hybrid gain medium, which included a purely homogeneous gain medium and a purely inhomogeneous gain medium, was modeled. The modeling was

based on the intensity growth rate equations and small change of the intensity during one round trip so that the stability near equilibrium can be determined. The stable operation of the multi-wavelength laser can be demonstrated theoretically and experimentally. Twenty-two stable wavelengths within a bandwidth of 3 dB were obtained in the ring laser having an Erbium Doped Fiber Amplifier (EDFA) and a Semi-conductor Optical Amplifier (SOA). Because of low noise performance of the EDFA, the oscillation bandwidth, Signal to Noise Ratio and power can be enhanced when comparing this ring laser with an SOA ring laser.

5.2 Further Work

Further studies of the comb filter and the gain medium are suggested. A stable and tunable comb filter is discussed first so as to build a tunable multiwavelength fiber laser, which vitalizes the development of the optical communication and optical fiber sensing. Next, the interaction between a 1480 nm pump laser and a Semi-conductor Optical Amplifier (SOA) in the hybrid gain medium is discussed. Finally, investigation of the hybrid gain medium, which is formed by the L-band EDFA and the SOA in the laser cavity, is suggested.

5.2.1 Comb Filter

The comb filters fix the wavelength spacing in the multi-wavelength fiber laser. They are commonly formed by means of the interferometric technique. However, they always suffer from the wavelength drift of phase induced by environmental perturbation. This causes the drift of comb pattern in an optical spectrum. In order to have a stable output of the multi-wavelength fiber laser, stabilization of the interferometers is required.

Two stabilizing control loops are suggested working in the multi-wavelength fiber laser with hybrid gain medium. Actually, there are two interferometers with different optical path differences in the laser cavity. One of the interferometers fixes the wavelength spacing while the other acts as a bandpass filter whose bandwidth is at least 20 times larger than the wavelength spacing. By tuning the centers of wavelengths in the comb patterns of the two interferometers respectively, the tunable multiwavelength laser can be built.

The working principles of both control loops are exactly the same. In the control loop, a Fiber Bragg Grating (FBG) filters one of the lasing wavelengths from the laser output. The wavelength drift of the output induces an intensity change in the FBG. A

photodetector converts an optical signal to an electrical signal. In a differential amplifier, the electrical signal corresponding to the intensity change is compared with a reference voltage source so as to obtain an error signal. It is subsequently sent to an integration controller which generates a corrective signal. Finally, it is delivered to the PZT of the interferometers after passing through an electrical amplifier. Such a process continuously operates in order to minimize the wavelength drift of the laser output with frequency up to MHz.

In fact, a Bragg wavelength of the FBG acts as a reference point of the control loop. If uniform stress is exerted on the FBG, its Bragg wavelength will shift. Then, the control loop tunes the center of wavelength of the comb pattern in the interferometer to a new reference point. Finally, the lasing wavelength of laser output can also be tuned by means of exerting the uniform stress on the FBGs in the two control loops respectively.

5.2.2 Gain medium

Researches on the multiwavelength fiber laser are concerned with how to increase the number of lasing wavelengths and to operate the fiber laser at room temperature. This may always be related to the properties of the gain medium in the

fiber laser such as homogeneous broadening and inhomogeneous broadening.

In chapter 4, the fiber laser with hybrid gain medium was proposed. It is also investigated experimentally and theoretically. However, the theoretical model is only valid near equilibrium. The theoretical conclusion is still missing within transient period. Moreover, the interaction between the 1480 nm pump laser and the SOA is not included in such a model. In fact, the 1480 nm pump laser accelerates the gain recovery in the SOA and enhances the saturation output power. This may assist to further suppress the mode competition in the fiber lasers with a practical hybrid gain medium. In order to further explore the properties of such a hybrid gain medium and to verify the suppression of the mode competition by injecting the 1480 nm pump laser to the SOA, the detailed theoretical analysis based on Semi-Classical theory is worthy of doing.

In Fig. (4.7), the oscillation bandwidth of such a fiber laser with the hybrid gain medium is ranged from the end of the C-band to the beginning of the L-band. Obviously, the gain supported by C-band EDFA is so low within the spectrum near L-band. In order to widen the oscillation bandwidth and to increase the power of laser output, the gain of the fiber laser may be required to boost up. The straightforward

approach is to replace the C-band EDFA with the L-band EDFA. The pumping power in the L-band EDFA is required to adjust carefully in the hybrid gain medium so that an optimum spectrum of laser output is obtained. If the pumping power is too weak, the absorption from the L-band EDFA will reduce the net gain of the fiber lasers. However, high gain supported by the L-band EDFA may suppress the oscillation bandwidth because the homogeneous broadening is dominant in the hybrid gain medium.

Thhe Hœ

g KPloytcoi UvorcU

1. D. N. Wang, F. W. Tong, Xiaohui Fang, W. Jin, P. K. A. Wai and J. M. Gong, "Multiwavelength Erbium-doped Fiber Ring Laser Source with a Hybrid Gain Medium", *Optics Communications*, (communicating with reviewers)

2. D. N. Wang, F. W. Tong, Xiaohui Fang, W. Jin, P. K. A. Wai and J. M. Gong, "Multiwavelength Fiber Laser Source with a Hybrid Gain Medium" accepted by *The 23rd annual Conference on Lasers and Electro-Optics (CLEO 2003)*

3. F. W. Tong, D. N. Wang, J. M. Gong, W. Jin and P. K. A. Wai, "A Multiwavelength Fiber Laser Operated at room temperature", *The seventh Optoelectronics and Communications Conference (OECC 2002)*, pp. 281-282, 2002

4. F. W. Tong, D. N. Wang, H. Li and W. Jin, "A Dual-Band Multiwavelength Erbium-Doped Fiber Laser Source", *Microwave and Optical Technology Letters*, vol. 32, pp.458-461, 2002